TABLE I – SUMMARY OF CLINICAL CHARACTERISTICS OF OVARIAN CANCER PATIENTS EXAMINED IN THIS STUDY

Histology	Mean age (range)	FIGO stages				Total
		I	II	III	IV	
CCC	53 (36–66)	27	5	9	2	43
Endometrioid	53 (28–66)	2	7	4	0	13
Mucinous	53 (28–90)	6	1	1	0	8
SAC	55 (33–81)	9	13	35	5	62
						126

Obstetricians) classification system. Patient profiles (age, FIGO stage) were analyzed against each of the 4 major epithelial ovarian cancer histological types (CCC, endometrioid adenocarcinoma, mucinous adenocarcinoma and serous adenocarcinoma). Written informed consent was obtained for all the cases, and the experimental protocol was approved by the ethics committee of Osaka University.

Cell lines

Human clear cell carcinoma (CCC) ovarian cancer cell lines (OVISE, OVTOKO, OVMANA and RMG-1) and serous adenocarcinoma (SAC) ovarian cancer cell lines (OVSAHO and OVKATE) were obtained from the Japanese Collection of Research Bioresources (JCRB, Osaka, Japan). Cells were maintained in RPMI 1640 medium supplemented with 10% fetal bovine serum (FBS) (HyClone Laboratories, Logan, UT) and 1% penicillin–streptomycin (Nacalai Tesque, Kyoto, Japan) at 37°C under a humidified atmosphere of 5% CO_2.

Protein extraction and 2D-DIGE

Proteins extracts of the cell lines were prepared with the Complete Mammalian Proteome Extraction Kit (Calbiochem, La Jolla, CA) and stored at −80°C until use. Protein concentrations were determined with the RC-DC Protein Assay kit (Bio-Rad Laboratories, Hercules, CA) using BSA as the standard. Before 2D-DIGE, we performed fluorescence labeling, for which the OVISE and OVSAHO samples were labeled with Cy3 and Cy5 CyDye DIGE fluorminimal dyes (GE Healthcare Bio-Sciences, Little Chalfont, Buckinghamshire, UK), respectively. For first-dimension separation, isoelectric focusing electrophoresis was performed using ReadyStrip™ (Bio-Rad Laboratories) IPG strips (24 cm, pH3-10NL). The labeled proteins (150 μg) were then loaded onto a gel strip, which was rehydrated in the dark for 12 hr (99,000 Vh) with the labeled protein sample diluted to 430 μl with a rehydration buffer (7 M urea, 2 M thiourea, 4% CHAPS, 2 mM TBP, 0.0002% BPB, 1.0% Bio-lyte 3-10 and 1.2% destreak). After isoelectric focusing, proteins were reduced in an equilibration buffer (50 mM Tris-HCl containing 6 M urea, 20% v/v glycerol and 2% SDS, pH 8.8) containing 20 mg/ml DTT for 40 min followed by carbamidomethylation in the equilibration buffer containing 25 mg/ml iodoacetamide for 30 min in the dark. The second-dimension separation was performed on 10% polyacrylamide gels using the EttanDalt-Six system (GE Healthcare Bio-Sciences) at a constant wattage of 100 W at 20°C for 3 hr. Gel electrophoresis was performed in the dark, and the gels were scanned with the Typhoon scanner (GE Healthcare Bio-Sciences).

Protein identification by mass spectrometry

2D-PAGE was performed in parallel with 2D-DIGE using OVISE and OVSAHO protein extracts without fluorescence labeling. Gels were stained using a Silver Stain MS Kit (WAKO Pure Chemical Industries, Ltd., Osaka, Japan). Protein spots in a silver-stained gel, corresponding to the spots of interest in the 2D-DIGE scanned image, were digested in gel according to a previously described method,[16] using sequencing grade modified trypsin (Promega, Inc., Madison, WI). Digested peptides were then extracted with 5% TFA in acetonitrile (ACN/DW 50:45), sonicated for 5 min and concentrated by evaporation. The peptides were solubilized with 0.1% TFA in ACN/DW (2:98) and analyzed by means of LC-MS/MS. For reverse-phase separations, a Magic 2002 capillary HPLC (Michrom BioResources, Auburn, CA) with a C-18 RP column (length 15 cm, i.d. 200 μm; GL Sciences Inc., Tokyo, Japan) was used. The injected peptides were then eluted with a 30-min linear gradient of 5–65% of solvent B (solvent A: 0.1% formic acid in ACN/DW, 2:98; solvent B: 0.1% formic acid in ACN/DW, 95:5). The column was directly interfaced to an LCQ ion trap mass spectrometer (ThermoElectron, San Jose, CA) equipped with a nanoelectrospray ion source, and data were collected in the double mode that was configured to alternate between a single full MS scan and an MS/MS scan of the most intense precursor masses. MS/MS spectra were searched against the human protein Swiss-Prot database with the aid of the MASCOT search program (version 2.1.03; Matrix Science K.K., Tokyo, Japan). The following parameters were used for the search: enzyme: trypsin, missed cleavage; 1, variable modification; oxidation of methionines, fixed modification; carbamidomethylation of cysteins and monoisotopic peptide masses.

Real-time RT-PCR

For the quantification of Anx A4 mRNA in different ovarian cancer cell lines (CCC and SAC), we performed real-time RT-PCR. Total RNA was prepared from OVISE, OVTOKO, OVMANA, RMG-1 (CCC), OVSAHO and OVKATE (SAC) cell lines using an RNeasy Kit (Qiagen Valencia, CA) and cDNA was synthesized with a SuperScript™ III Reverse Transcriptase Kit (Invitrogen, Carlsbad, CA). A standard curve for Anx A4 cDNA was generated by the serial dilution of plasmid vector DNA, which encodes the Anx A4 gene. The primer sequences for Anx A4 were as follows: forward primer, 5′-ggaggtactgtcaaagctgc-3′ and reverse primer, 5′-gccactcagttctgacttcag-3′. Primers and cDNA were added to SYBR green premix (Invitrogen), which contained all the reagents required for PCR. The PCR conditions consisted of 1 cycle at 95°C for 1 min and 42 cycles of 95°C for 20 sec, 50°C for 20 sec and 72°C for 30 sec. PCR products were measured continuously with the My IQ™ Single-Color Real-Time Detection System (Bio-Rad Laboratories).

Western blotting

Cells and frozen tumor tissue samples were lysed in RIPA buffer (10 mM Tris-HCl, pH 7.5, 150 mM NaCl, 1% Nonidet P-40, 0.1% sodium deoxycholate, 0.1% SDS, 1 mM Na_3VO_4 and 1 × protease inhibitor cocktail (Nakalai Tesque)) followed by centrifugation (13,200 rpm, 4°C, 15 min), after which the supernatants were stored at −80°C until use. Protein concentrations were determined with the DC Protein Assay kit (Bio-Rad Laboratories), using BSA as the concentration standard. Extracted proteins were then resolved using 10% Bis-Tris Criterion XT Precast gels (Bio-Rad Laboratories) and subsequently transferred to PVDF membranes (Millipore, Bedford, MA). The membranes were washed and blocked with 1% skim milk in PBS containing 0.1% Tween 20 (PBST) and incubated with a goat polyclonal anti-Anx A4 antibody (sc-1930; Santa Cruz Biotechnology, Santa Cruz, CA) at a 1:300 dilution. Next, the membranes were incubated with horseradish peroxidase-conjugated donkey anti-goat IgG (Santa Cruz Biotechnology). Finally, the signals were visualized by means of an enhanced chemiluminescence (ECL) reaction system (Perkin-Elmer Life Sciences, Boston, MA). For loading control, western blotting and the subsequent antigen–antibody reaction were performed with GAPDH (Santa Cruz Biotechnology).

Immunohistochemistry

Expression of Anx A4 protein in ovarian cancer patient tissue sections was immunohistochemically measured with the ABC Kit (Vector Laboratories, Burlingame, CA). The total number of tissue section samples analyzed was 126 (43 CCC, 13 endometrioid, 8 mucinous, 62 SAC). Sections (3 μm) were prepared from formalin-fixed, paraffin-embedded tissue specimens, deparaffinized and rehydrated in graded alcohols. For antigen retrieval, the sections were incubated in a target retrieval solution (DAKO, Kyoto,

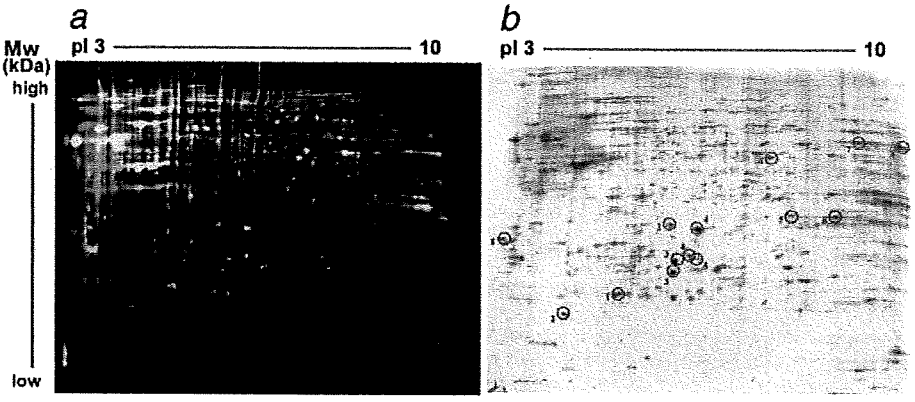

FIGURE 1 – Proteomic analysis of OVISE CCC and OVSAHO SAC cell lines. Representative gel images of 3 independent experiments are shown. A 2D-DIGE gel image of OVISE CCC and OVSAHO SAC cell lines is shown in (*a*). Green spots correspond to proteins upregulated in OVISE cells (Cy3 labeled) compared with OVSAHO cells (Cy5 labeled). Red spots correspond to proteins upregulated in OVSAHO cells (Cy5 labeled) compared with OVISE cells (Cy3 labeled). Yellow spots correspond to proteins expressed at the same level in the OVISE and OVSAHO cell lines. A corresponding silver stain gel image is shown in (*b*).

Japan) in a hot water bath at 98°C for 40 min. In brief, quenching endogenous peroxidase with 3% H_2O_2 in methanol for 20 min. After treatment with BlockAce (Dainippon Sumitomo Pharmaceutical, Osaka, Japan) for 30 min at room temperature, the sections were incubated with a goat polyclonal anti-Anx A4 antibody at 1:100 dilution at 4°C overnight and subsequently incubated with a biotinylated anti-goat IgG antibody (Vector Laboratories Inc.) at room temperature for 1 hr. The antibody complex was detected by incubation with an avidin-biotin-peroxidase complex solution (Vector Laboratories Inc.) and visualized with 3,3′-diaminobenzidine tetrahydrochloride (MERCK, Darmstadt, Germany). Tissue sections were counter-stained with hematoxylin. Three gynecologic oncologists (A.K., T.M., Y.U.), blinded to the histological data, reviewed the stained sections. Cases with >90% of tumor cells staining positively with the anti-Anx A4 antibody were considered strongly positive (+++), cases with >50% but <90% Anx A4-positive cells medium positive (++), those with <50% positive cells weakly positive (+) and those with no or hardly any positive cells were considered negative.

Construction of Anx A4 expression vector

Total RNA from OVISE cells was purified with an RNA-Bee solution (Tel-Test Inc., Friendswood, TX) and cDNA was prepared with a SuperScript™ III Reverse Transcriptase Kit (Invitrogen). To construct the Anx A4 expression vector, cDNA of human Anx A4 was amplified using KOD-plus (Toyobo Co. Ltd., Osaka, Japan) with the following primers: Anx A4 forward primer 5′-ttgacctagagtcatggcca-3′ and Anx A4 reverse primer 5′-tttaatcatctcctccacag-3′. The amplified cDNA was then inserted into pcDNA3.1/V5-His-TOPO vector (Invitrogen) and designated pcDNA3.1-Anx A4. The DNA sequence of Anx A4 cDNA inserted into the plasmid was confirmed using the ABI PRISM 3100 Genetic Analyzer (Applied Biosystems, Foster City, USA).

Generation of Anx A4 stable transfectant cells

To generate Anx A4 stable transfectant cells, the OVSAHO cell line was transfected with pcDNA3.1-Anx A4 using Lipofectamine 2000 (Invitrogen) according to the manufacturers' instructions, after which the cells were selected with 500 μg/ml of Geneticin (GIBCO, Invitrogen, Carlsbad, CA). We also transfected empty vector into the OVSAHO cell line using the same procedure described earlier to generate control cells. Stable clones were maintained in 250 μg/ml of Geneticin. Western blot analysis was performed to confirm the levels of Anx A4 expression in Anx A4 transfectant cells and empty vector control cells.

Measurement of IC_{50} values after carboplatin treatment

Anx A4 transfected OVSAHO cells and empty vector control cells were seeded in 96-well plates (3,000 cells/well) (Costar; Corning Inc., Corning, NY) for 24 hr and then exposed to various concentrations (0-150 μM) of carboplatin for 72 hr. The cells were incubated with 10 μl of Cell Counting Kit-8 (Dojindo, Osaka, Japan) in 100 μl RPMI-1640 medium for 3 hr. Absorbance at 450 nm was measured with a microplate reader (Bio-Rad Model 680), and absorbance values were expressed as percentages relative to those for untreated controls, and the concentrations resulting in 50% inhibition of cell growth (IC_{50} values) were calculated.

Measurement of intracellular platinum accumulation

Carboplatin accumulation in Anx A4 transfected cells and control cells was analyzed according to a previously established method[17] with minor modifications. In brief, 1.5×10^6 cells were seeded into a 60-mm tissue culture dish and incubated for 24 hr. The cells were then exposed to 2 mM carboplatin for 60 min at 37°C and washed twice with PBS either immediately or after 360 min of incubation in carboplatin-free RPMI 1640 medium supplemented with 10% FBS (HyClone Laboratories). After whole-cell extracts were prepared, the concentration of intracellular platinum was determined by using a polarized Zeeman atomic absorption spectrophotometer (model Z-8000; Hitachi, Ltd., Tokyo, Japan). The absolute concentration of platinum in each sample was determined from a calibration curve prepared with a platinum standard solution.

Statistical analysis

Student's *t* tests were used for statistical analyses. For the immunohistochemical analysis, a nonparametric analysis (the Kruskal–Wallis test) was used. A value of $p < 0.05$ was considered statistically significant.

Results

Anx A4 expression is elevated in CCC cell lines compared with SAC cell lines

The protein expression profiles of OVISE (CCC) and OVSAHO (SAC) cell lines were compared by means of 2D-DIGE analyses using fluorminimal dye-labeled protein extracts. The resulting gel images and corresponding silver-stained gels are shown in Figures 1*a* and 1*b*. Eight proteins highly expressed in OVISE cells and 6 proteins in OVSAHO cells were selected for identification by LC-MS/MS analysis. The results of these analyses (Table II) revealed

TABLE II – PROTEINS DIFFERENTIALLY EXPRESSED IN OVISE AND OVSAHO CELL LINES

Spot no.	Access. no.	Identified protein	M_w (Da)	pI	Coverage (%)
Proteins upregulated in OVISE cells compared with OVSAHO cells					
1	P09211	Glutathione S-transferase P	23,438	5.44	38
2	P09525	Annexin A4 (Annexin IV)	35,957	5.85	49
3	P04792	Heat-shock protein beta-1	22,826	5.98	39
4	Q13011	Delta3,5-delta2,4-dienoyl-CoA isomerase, mitochondrial precursor	36,136	8.16	28
5	P30040	Endoplasmic reticulum protein ERp29 precursor	29,032	6.77	15
6	O75874	Isocitrate dehydrogenase [NADP] cytoplasmic	46,915	6.53	39
7	P68104	Elongation factor 1-alpha 1	50,451	9.1	14
8	P68104	Elongation factor 1-alpha 1	50,451	9.1	19
Proteins upregulated in OVSAHO cells compared with OVISE cells					
1	Q07021	Complement component 1 Q subcomponent-binding protein, mitochondrial precursor	31,742	4.74	14
2	O75947	ATP synthase D chain, mitochondrial	18,405	5.22	41
3	P30084	Enoyl-CoA hydratase, mitochondrial precursor	31,823	8.34	27
4	P42126	3,2-trans-enoyl-CoA isomerase, mitochondrial precursor	33,080	8.8	10
5	P45880	Voltage-dependent anion-selective channel protein 2	38,639	6.32	25
6	P45880	Voltage-dependent anion-selective channel protein 2	38,639	6.32	25

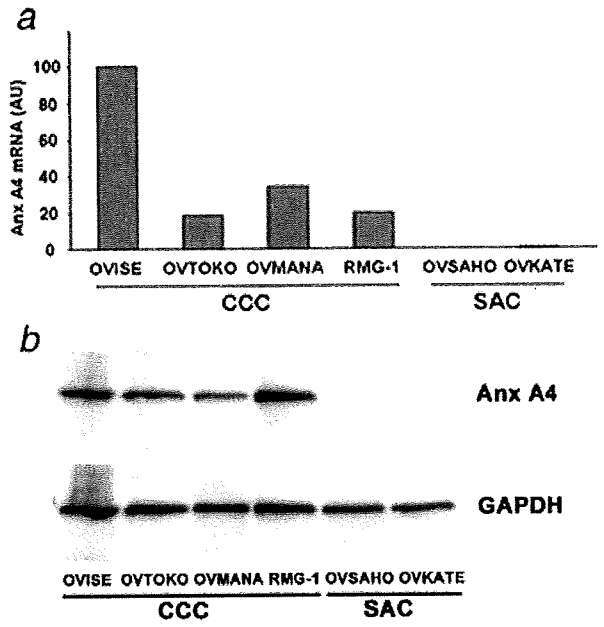

FIGURE 2 – Real-time RT-PCR and Western blot analysis of levels of Annexin A4 expression in ovarian cancer cell lines. Levels of Annexin A4 mRNA in ovarian CCC cell lines (OVISE, OVTOKO, OVMANA and RMG-1) and in ovarian SAC cell lines (OVSAHO and OVKATE) were determined by real-time RT-PCR (*a*). Levels of Annexin A4 protein in ovarian CCC cell lines (OVISE, OVTOKO, OVMANA and RMG-1) and in ovarian SAC cell lines (OVSAHO and OVKATE) were determined by Western blot analysis (*b*).

enhanced expression of the Anx A4 protein in the OVISE cell line compared with the OVSAHO cell line.

The specific overexpression of Anx A4 in ovarian CCC cell lines compared with that in SAC cell lines was further evaluated by real-time RT-PCR (Fig. 2*a*) and Western blot analysis (Fig. 2*b*). As shown in Figure 2*a*, expression of Anx A4 (mRNA level) in OVISE, OVTOKO, OVMANA and RMG-1 (CCC) cell lines was enhanced compared with the OVSAHO and OVKATE (SAC) cell lines where Anx A4 expression (mRNA level) was barely detectable. Western blot analysis (Fig. 2*b*) also demonstrated enhanced expression of Anx A4 (protein level) in OVISE, OVTOKO, OVMANA, RMG-1 (CCC) cell lines compared with the OVSAHO and OVKATE (SAC) cell lines.

Enhanced expression of Anx A4 protein in tumors of ovarian CCC patients

Next, we determined whether levels of Anx A4 protein are elevated in tumors of patients with ovarian CCC compared with other ovarian cancers. For this analysis, we performed an immunohistochemical study of Anx A4 expression in tumor tissue samples from a large cohort of ovarian cancer patients (126 patients in total). In addition, we performed Western blot analysis using several frozen tumor tissue samples and compared the results with those of the immunohistochemical study. Representative immunohistochemical staining of Anx A4 in tissue sections from patients with ovarian cancer revealed intense Anx A4 staining in ovarian CCC compared with other histological types (Fig. 3*a*). Positive staining scores for Anx A4 in tissue sections from patients with other types of ovarian cancers are shown in Figure 3*b*. We observed significantly stronger ($p < 0.01$) positive staining in tissue sections from patients with ovarian CCC compared with patients with ovarian endometrioid and serous adenocarcinoma. Of 43 CCC tissue sections, more than 30 were strongly positive for Anx A4 (+++) compared with only 5 of the 62 SAC samples. Western blot analysis showed enhanced expression of Anx A4 in CCC tumor samples that had demonstrated strong Anx A4 immunohistochemical staining (+++) but barely detectable expression of Anx A4 in SAC tumor samples that had demonstrated negative (−) Anx A4 immunohistochemical staining (Fig. 3*c*).

Transfection of Anx A4 cDNA into ovarian cancer cells enhances resistance to carboplatin treatment and modulates drug cellular efflux

Because Anx A4 has been demonstrated to perform a functional role in chemoresistance in some cancer cell lines,[14] we determined whether Anx A4 can also confer chemoresistance to epithelial ovarian cancer cells. For this study, we generated Anx A4 stably transfected OVSAHO cells. Figure 4*a* shows a Western blot analysis of Anx A4 levels in OVSAHO parent cells, Anx A4 stably transfected OVSAHO cells and empty vector transfected control cells. Figure 4*b* shows cell survival plots for control and OVSAHO/Anx A4 cell lines after treatment with increasing concentrations of carboplatin (0–150 μM). From this analysis, we determined the IC_{50} carboplatin concentration values for the 2 cell lines. Higher (approximately double) IC_{50} carboplatin concentration was observed in the OVSAHO/Anx A4 (IC_{50} = 42 μM) cells compared with the empty vector control cells (IC_{50} = 23 μM). These results demonstrate that Anx A4 can confer chemoresist-

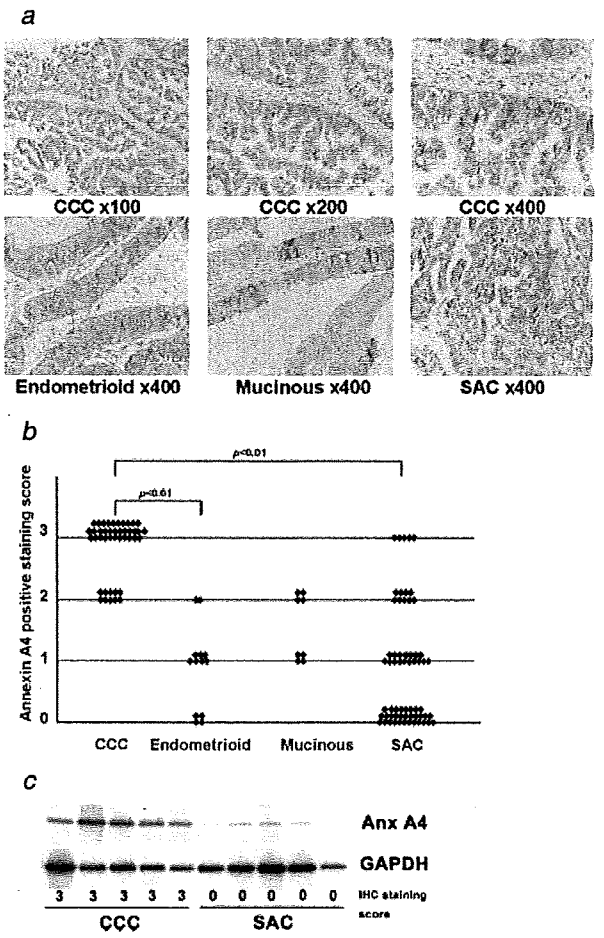

FIGURE 3 – Immunohistochemical analysis of Annexin A4 in ovarian cancer tumors. Levels of Annexin A4 protein in 126 epithelial ovarian cancer samples were determined by immunohistochemical analysis. Representative images of tissue sections from CCC (n = 43), endometrioid (n = 8), mucinous (n = 13) and serous adenocarcinoma (n = 62) ovarian cancer patients after immunohistochemical staining for Annexin A4 (*a*). Annexin A4-positive staining scores of tissue sections from ovarian cancer tumors (*b*). The p value between CCC and SAC is provided as determined by the nonparametric Kruskal–Wallis test. Western blot analysis using 5 CCC frozen tumor samples and 5 SAC frozen tumor samples (*c*).

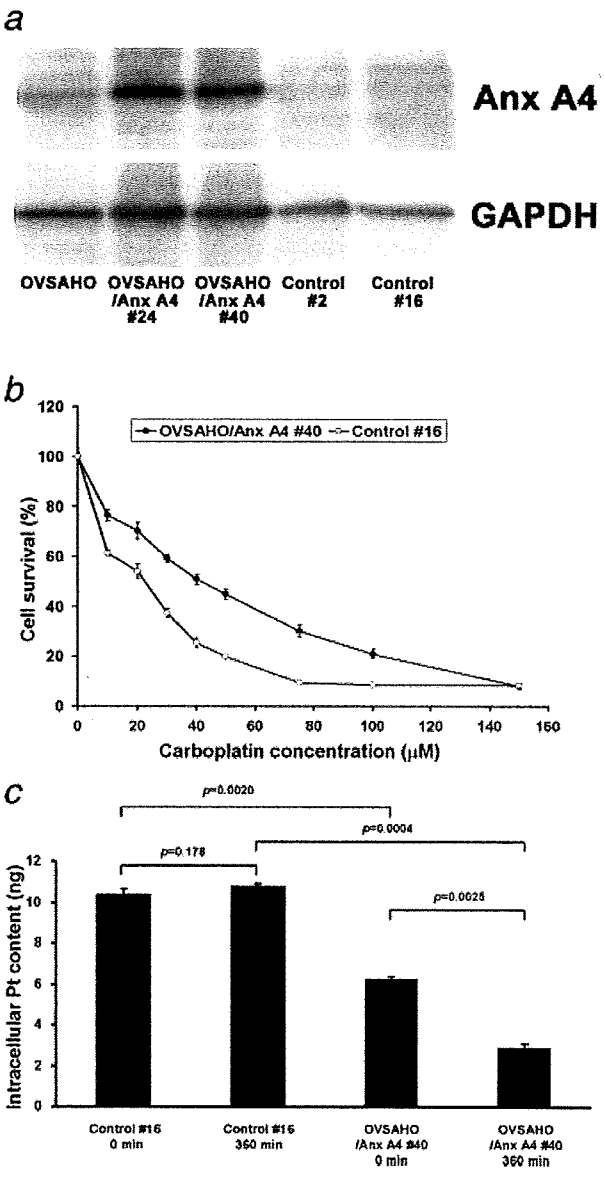

FIGURE 4 – Transfection of Annexin A4 cDNA into ovarian cancer cells confers resistance to carboplatin and decreases intracellular Pt accumulation. Cell survival (expressed as a percentage relative to control untreated cells) after 72 hr treatment of OVSAHO/Anx A4 and empty vector control cells with different concentrations of carboplatin (Figure 4*a*). The obtained IC50 values were 42 μM for OVSAHO/Anx A4 no. 40 and 23 μM for Control no. 16 (not shown in figure). Intracellular platinum content after treatment with 2 mM carboplatin for 60 min with or without after 360 min of incubation in carboplatin-free medium in OVSAHO/Anx A4 cells and control cells, as determined by atomic absorption spectrophotometry (Figure 4*c*).

ance in ovarian cancer cells. To investigate the molecular mechanisms of chemoresistance induced by Anx A4, we quantitated the intracellular platinum content after treatment of OVSAHO/Anx A4 and empty vector control cells with carboplatin. Figure 4*c* shows an analysis of intracellular platinum accumulation in OVSAHO/Anx A4 cells and empty vector control cells after carboplatin treatment with or without an additional incubation time (360 min) in carboplatin-free medium. Significantly (p = 0.0020) reduced levels of intracellular platinum accumulation were noted in OVSAHO/Anx A4 cells (OVSAHO/Anx A4 no. 40, 0 min) compared with empty vector control cells (Control no. 16, 0 min) when neither cell line underwent additional incubation in carboplatin-free medium. Control cells displayed no significant difference (p = 0.178) in intracellular platinum content between 0 min and 360 min of additional carboplatin-free incubation time (Control no. 16, 0 min *vs.* Control no. 16, 360 min), whereas OVSAHO/Anx A4 cells showed a significant decrease (p = 0.0025) in intracellular platinum content at 360 min as compared with at 0 min of additional carboplatin-free incubation time (OVSAHO/Anx A4 no. 40, 0 min *vs.* OVSAHO/Anx A4 no. 40, 360 min). Furthermore, OVSAHO/Anx A4 cells displayed significantly decreased (p = 0.0004) levels of intracellular platinum con-

tent compared with control cells after an additional 360 min of carboplatin-free incubation (Control no. 16, 360 min *vs.* OVSAHO/Anx A4 no. 40, 360 min), which suggests a role for Anx A4 in enhancing cellular platinum efflux.

Discussion

The use of carboplatin and paclitaxel for the treatment of ovarian cancers has significantly improved survival rates in patients with this disease.[18] However, of the 4 major histological types of ovarian cancer, CCC of the ovary is characterized by strong chemoresistance.[2] Consequently, patients with this disease are associated with significantly lower 5-year survival rates than patients with other histological types of ovarian cancer.[19,20] However, the molecular mechanisms of chemoresistance in this disease have remained poorly understood. Thus, the identification of proteins which are involved in chemoresistance in ovarian CCC is of major clinical importance because these proteins may constitute novel therapeutic targets in this disease.

In this study, we performed a 2D-DIGE proteomic analysis using ovarian cancer cell lines for the identification of a candidate protein associated with chemoresistance in ovarian CCC. We identified 8 proteins differentially upregulated in OVISE CCC cells compared with OVSAHO SAC cells (Table II). From among those 8 proteins, we focused on Anx A4, a calcium-dependent phospholipid-binding protein, which is localized proximal to the cell membrane and plays an important role in membrane fluidity or trafficking.[10]

We confirmed by means of both real-time RT-PCR (mRNA levels) and Western blot analysis (protein levels) that expression of Anx A4 was significantly enhanced in ovarian CCC cell lines compared with in non-CCC ovarian cancer cell lines (Figs. 2*a* and 2*b*). The findings of our analysis using ovarian cancer cell lines are in agreement with those of the proteomic study of Morita *et al.*,[15] in which Anx A4 was identified as being differentially upregulated in ovarian CCC cell lines (OVISE and OVTOKO) compared with an ovarian mucinous cancer cell line.

Previous studies have associated Anx A4 protein with chemoresistance. For example, in a study of Han *et al.*,[14] Anx A4 was observed to be elevated in a paclitaxel-resistant human lung cancer cell line and transfection of Anx A4 cDNA into embryonic kidney 293T cells to confer resistance to paclitaxel. Because Anx A4 has been shown to be involved in modulating membrane permeability and membrane trafficking,[10] it is conceivable that this involvement may result in modulation of both cellular drug influx and efflux after chemo-drug treatment. Taken together, these studies suggest that the strong chemoresistance characteristic of human ovarian CCC may be due to enhanced expression of Anx A4. However, it remained unclear whether levels of Anx A4 protein are significantly elevated in tumors of patients with ovarian CCC compared with other histological types.

In the study reported here, we, therefore, performed an immunohistochemical analysis of Anx A4 in tumor tissue samples from 126 patients with epithelial ovarian cancer to determine whether levels of Anx A4 protein are elevated in tumors of patients with ovarian CCC compared with other epithelial ovarian cancers. Because treatment with paclitaxel can enhance Anx A4 expression in cultured cells,[14] all patients examined in this analysis had undergone preliminary diagnosis and had not received chemotherapy (including carboplatin or paclitaxel) before surgery. The results of this analysis revealed significantly ($p < 0.01$) strong positive staining (enhanced expression) of Anx A4 in tumor tissue samples from patients with ovarian CCC compared with endometrioid and serous adenocarcinoma, which are known to represent chemosensitive histological types (Fig. 3*b*). Western blot analysis using frozen tumor samples were compatible with results of the IHC study (Fig. 3*c*). Thus, our study was able to demonstrate the presence of enhanced expression of Anx A4 in tumors of patients with ovarian CCC. This finding is in agreement with that of our proteomic analysis using ovarian cancer cell lines and indicates that Anx A4 may play a role in tumor resistance to cancer chemotherapy in patients with ovarian CCC.

To investigate a relationship between levels of expression of Anx A4 and patient prognosis, we reviewed clinical outcomes (recurrence, progression-free survival, etc.) of the 62 SAC patients including 5 patients with strong (+++)Anx A4 povitive staining in IHC analysis. Among the 5 SAC patients with high levels of Anx A4 expression, 2 patients are well and alive with no recurrence, whereas the other 2 patients have recurred within 1 or 2 years after treatment and 1 patient was out of follow-up. We have compared the progression-free survival between these 5 patients and Anx A4 negative SAC patients and there was no statistically significant difference between the 2 groups. Because the number of Anx A4-positive SAC patients is small, further investigation will be necessary in a larger cohort of patients.

Although previous studies have demonstrated a role for Anx A4 in conferring chemoresistance to human cancer cell lines,[14] a similar role in human epithelial ovarian cancer cells was not identified, and the specific mechanism of chemoresistance that Anx A4 confers was not previously determined. Therefore, we first studied cell survival after carboplatin treatment to confirm whether Anx A4 can enhance chemoresistance in epithelial ovarian cancer cells. We were unable to reduce Anx A4 protein levels in the OVISE CCC cell line, despite using various strategies (including siRNA), which may be due to the reported long half-life of Anx A4 protein (approximately 4 days).[21] We then tested the effect of forced overexpression of Anx A4 in the OVSAHO non-CCC (SAC) ovarian cancer cell line in which Anx A4 is not endogenously expressed. We observed enhanced chemoresistance to carboplatin treatment in cells that stably expressed Anx A4 compared with empty vector control cells (Figs. 4*a* and 4*b*). Thus, our results demonstrate that Anx A4 protein plays a role in the enhancement of chemoresistance in epithelial ovarian cancer cells.

We next examined intracellular platinum accumulation in both Anx A4 expressing ovarian cancer cells (OVSAHO/Anx A4 cells) and empty vector control cells after carboplatin treatment (Fig. 4*c*). Our results of carboplatin treatment with no carboplatin-free incubation revealed significantly reduced levels of intracellular platinum content in OVSAHO/Anx A4 cells compared with control cells, which indicates that Anx A4 inhibits cellular platinum influx and/or promotes cellular platinum efflux. Comparison of the results for 0 and 360 min carboplatin-free incubation showed that OVSAHO/Anx A4 cells are more active in promoting cellular platinum efflux compared with control cells. Taken together, these results demonstrate that Anx A4 plays a part in the enhancement of cellular platinum efflux.

Our study has demonstrated for the first time elevated levels of Anx A4 protein in patients with ovarian CCC and an association between elevated Anx A4 levels and enhanced chemoresistance to carboplatin in human epithelial ovarian cancer cells. It has also found evidence for the first time that Anx A4 confers chemoresistance in part by enhancing drug efflux. Thus, it is conceivable that the observed strong resistance to cancer chemotherapy (including carboplatin) specific to ovarian CCC tumors, compared with that of other epithelial ovarian tumors, is mediated through the enhanced expression of Anx A4 in patients with this disease. Therefore, Anx A4 may constitute a novel therapeutic target for overcoming resistance to cancer chemotherapy in patients with ovarian CCC. In view of the reported half-life of Anx A4 protein, such a therapeutic strategy is likely to involve the inhibition of the function rather than of the expression of Anx A4 in patients with CCC.

Acknowledgements

The authors are grateful for experimental assistance from Ms. Y. Matsukawa and for secretarial assistance from Ms. Y. Ito and Ms. N. Kawakami.

References

1. Jemal A, Siegel R, Ward E, Hao Y, Xu J, Murray T, Thun MJ. Cancer statistics, 2008. CA Cancer J Clin 2008;58:71–96.
2. Itamochi H, Kigawa J, Terakawa N. Mechanisms of chemoresistance and poor prognosis in ovarian clear cell carcinoma. Cancer Sci 2008; 99:653–8.
3. Jacobs IJ, Menon U. Progress and challenges in screening for early detection of ovarian cancer. Mol Cell Proteomics 2004;3:355–66.
4. Rapkiewicz AV, Espina V, Petricoin EF, III, Liotta LA. Biomarkers of ovarian tumours. Eur J Cancer 2004;40:2604–12.
5. Sugiyama T, Kamura T, Kigawa J, Terakawa N, Kikuchi Y, Kita T, Suzuki M, Sato I, Taguchi K. Clinical characteristics of clear cell carcinoma of the ovary: a distinct histologic type with poor prognosis and resistance to platinum-based chemotherapy. Cancer 2000;88: 2584–9.
6. Pectasides D, Pectasides E, Psyrri A, Economopoulos T. Treatment issues in clear cell carcinoma of the ovary: a different entity? Oncologist 2006;11:1089–94.
7. Kaetzel MA, Hazarika P, Dedman JR. Differential tissue expression of three 35-kDa annexin calcium-dependent phospholipid-binding proteins. J Biol Chem 1989;264:14463–70.
8. Zanotti G, Malpeli G, Gliubich F, Folli C, Stoppini M, Olivi L, Savoia A, Berni R. Structure of the trigonal crystal form of bovine annexin IV. Biochem J 1998;329:101–6.
9. Kaetzel MA, Mo YD, Mealy TR, Campos B, Bergsma-Schutter W, Brisson A, Dedman JR, Seaton BA. Phosphorylation mutants elucidate the mechanism of annexin IV-mediated membrane aggregation. Biochemistry 2001;40:4192–9.
10. Hill WG, Kaetzel MA, Kishore BK, Dedman JR, Zeidel ML. Annexin A4 reduces water and proton permeability of model membranes but does not alter aquaporin 2-mediated water transport in isolated endosomes. J Gen Physiol 2003;121:413–25.
11. Sohma H, Creutz CE, Gasa S, Ohkawa H, Akino T, Kuroki Y. Differential lipid specificities of the repeated domains of annexin IV. Biochim Biophys Acta 2001;1546:205–15.
12. Piljic A, Schultz C. Annexin A4 self-association modulates general membrane protein mobility in living cells. Mol Biol Cell 2006;17: 3318–28.
13. Kaetzel MA, Chan HC, Dubinsky WP, Dedman JR, Nelson DJ. A role for annexin IV in epithelial cell function. Inhibition of calcium-activated chloride conductance. J Biol Chem 1994;269:5297–302.
14. Han EK, Tahir SK, Cherian SP, Collins N, Ng SC. Modulation of paclitaxel resistance by annexin IV in human cancer cell lines. Br J Cancer 2000;83:83–8.
15. Morita A, Miyagi E, Yasumitsu H, Kawasaki H, Hirano H, Hirahara F. Proteomic search for potential diagnostic markers and therapeutic targets for ovarian clear cell adenocarcinoma. Proteomics 2006;6: 5880–90.
16. Shevchenko A, Wilm M, Vorm O, Mann M. Mass spectrometric sequencing of proteins silver-stained polyacrylamide gels. Anal Chem 1996;68:850–8.
17. Ikuta K, Takemura K, Sasaki K, Kihara M, Nishimura M, Ueda N, Naito S, Lee E, Shimizu E, Yamauchi A. Expression of multidrug resistance proteins and accumulation of cisplatin in human non-small cell lung cancer cells. Biol Pharm Bull 2005;28:707–12.
18. Paclitaxel plus carboplatin versus standard chemotherapy with either single-agent carboplatin or cyclophosphamide, doxorubicin, and cisplatin in women with ovarian cancer: the ICON3 randomised trial. Lancet 2002;360:505–15.
19. Tammela J, Geisler JP, Eskew PN, Jr, Geisler HE. Clear cell carcinoma of the ovary: poor prognosis compared to serous carcinoma. Eur J Gynaecol Oncol 1998;19:438–40.
20. O'Brien ME, Schofield JB, Tan S, Fryatt I, Fisher C, Wiltshaw E. Clear cell epithelial ovarian cancer (mesonephroid): bad prognosis only in early stages. Gynecol Oncol 1993;49:250–4.
21. Raynal P, Pollard HB, Srivastava M Cell cycle and post-transcriptional regulation of annexin expression in IMR-90 human fibroblasts. Biochem J 1997;322:365–71.

Gynecologic Oncology 113 (2009) 200–204

Contents lists available at ScienceDirect

Gynecologic Oncology

journal homepage: www.elsevier.com/locate/ygyno

The activity of carboplatin and paclitaxel for recurrent cervical cancer after definitive radiotherapy☆

Seiji Mabuchi *, Kenichirou Morishige, Masami Fujita, Tateki Tsutsui, Masahiro Sakata, Takayuki Enomoto, Tadashi Kimura

Department of Obstetrics and Gynecology, Osaka University Graduate school of Medicine. 2–2 Yamadaoka, Suita Osaka, 565–0871 Japan

ARTICLE INFO

Article history:
Received 17 October 2008
Available online 6 March 2009

Keywords:
Recurrent cervical cancer
Carboplatin–paclitaxel
Nedaplatin
Cisplatin
Radiotherapy

ABSTRACT

Objectives. The aim of this study was to evaluate the efficacy of paclitaxel–carboplatin (TC) for recurrent cervical cancer after definitive radiotherapy and to compare the results with non-taxane containing platinum-based chemotherapies (NTP).

Methods. The records of 59 consecutive women who had undergone salvage chemotherapy with TC ($n=28$) or NTP (historical control, $n=31$) for recurrence after definitive radiotherapy were retrospectively reviewed. Primary disease and recurrence data was collected. The activity and toxicity of TC were compared with those of NTP. The response rate and progression-free survival (PFS) after recurrence were the main endpoints. Multivariate analysis of prognostic factors for response was performed using the Cox proportional hazards regression model. Survival was calculated using the Kaplan–Meier methods and compared by the log-rank test.

Results. Overall, TC was well tolerated with a response rate of 67.9% (5 CR and 14 PR). The median PFS was 7 months for all patients and 10 months for responders. Myelosuppression was the most common toxicity (grade 3 in 16 patients, grade 4 in 5 patients). On the contrary, NTP showed a response rate of 22.6% with median and mean PFS of 0 month and 2 months, respectively. When compared, TC was significantly superior to NTP with regard to its response rate ($p=0.001$) and PFS ($p<0.0001$). Moreover, TC showed significantly higher activity in patients with adenocarcinoma histology.

Conclusions. Carboplatin–paclitaxel is active and well tolerated in patients with recurrent cervical cancer after definitive radiotherapy. This combination should be considered as an alternative regimen to cisplatin–paclitaxel in this patient population.

Introduction

Radiotherapy is the major treatment modality for invasive cervical cancer and can achieve a good treatment outcome in patients with early-stage disease. However, substantial treatment failure has been reported to occur in patients with advanced disease [1]. The recurrence rate is reported to be 10–20% in patients with FIGO stages Ib–IIa, compared to 50–70% in stage IIb–IVa patients [2].

Historically, cisplatin has been the most active single agent for recurrent cervical cancer. However, its response rate has been generally low, varying from 17% to 38% with a response duration of 3 to 6 months [3]. Moreover, according to a previous report [4], recurrences inside the irradiated field showed a lower response to cisplatin than recurrences outside the irradiated field (21% vs 73%, $p=0.0007$). Therefore, patients with recurrence after radiotherapy who are not amendable to the surgical resection or salvage radiotherapy (e.g. interstitial brachytherapy) have a dismal prognosis with a reported 1-year survival rate between 15% and 20% [5].

In order to improve survival, various studies have evaluated the survival benefit of adding other cytotoxic agents to cisplatin. A Gynecologic Oncology Group (GOG) phase III trial (protocol GOG 169) demonstrated that cisplatin–paclitaxel (TP) improves not only the response rate over single-agent cisplatin but also the progression-free survival in patients with advanced or recurrent cervical cancer [6]. Despite the improved clinical outcomes, the potentially severe gastrointestinal or neurologic toxicities of this regimen and the need for hospitalization may limit its use.

Since the objective of treatments for recurrent cervical cancer is the prolongation of survival and the maintenance of quality of life, the substitution of carboplatin for cisplatin may be beneficial. Single-agent carboplatin has been shown to have significant activity against recurrent cervical cancer with a response rate of 15–28.2% [7,8]. Different from cisplatin, the dose of carboplatin can be tailored

Abbreviations: AUC, Area under the curve; OS, Overall survival; DFI, Disease free interval; PFS, Progression-free survival; SCC, Squamous cell carcinoma.

☆ Grant support: This work was supported in part by a Grant-in-aid for Young Scientists (No 19890125) from the Ministry of Education, Culture, Sports, Science, and Technology of Japan, and a Grant-in-aid for General Scientific Research (No 19390429).

* Corresponding author. Fax: +81 6 6879 3359.
E-mail address: smabuchi@gyne.med.osaka-u.ac.jp (S. Mabuchi).

0090-8258/$ – see front matter © 2009 Elsevier Inc. All rights reserved.
doi:10.1016/j.ygyno.2009.02.008

according to renal function [9]. In addition, carboplatin has a more favorable non-hematologic toxicity profile [10]. However, although the combination of carboplatin–paclitaxel (TC) has been demonstrated to be equally efficacious to cisplatin–paclitaxel (TP) with less toxicity in patients with ovarian cancer [10], experience with the use of this combination in uterine cervical cancer is limited.

The use of TC in patients with cervical cancer was first reported in 1996 by Termrungruanglert et al. [11]. However, no controlled clinical trial has been conducted to evaluate the efficacy of TC in patients with recurrent cervical cancer. So far, only five retrospective studies on the value of TC with 3–48 recurrent or advanced cervical cancer patients have been reported, and they described response rates of 20–60% [12–16]. Moreover, the patient backgrounds in these articles were not uniform. Some were treated with TC for stage IV disease as a primary treatment, while others were treated for recurrence after either radiotherapy or surgical treatment (Table 1).

Based on a clinical trial that demonstrated the survival benefit of TP [6], the results of retrospective studies that evaluated the efficacy of TC (Table 1) and reported improvements in tolerability and patient convenience by substitution of TP for TC in ovarian cancer [10], we have started to use TC for patients with recurrent cervical cancer since 2005. In the current study, we conducted a retrospective analysis to evaluate the efficacy of TC against recurrent cervical cancer after definitive radiotherapy and compared the results with those from non-taxane containing regimens with regard to response rate and progression-free survival (PFS).

Materials and methods

Patients

Permission to proceed with data acquisition and analysis was obtained from the Osaka University Hospital's institutional review board. A list of patients who had received chemotherapy for recurrent cervical cancer at Osaka University Hospital from 1998 to 2008 was generated from our institutional pharmacy database. Then, through a chart review, patients that had been treated with carboplatin and paclitaxel were identified and retrospectively reviewed. Only patients with recurrent cervical carcinoma after definitive radiotherapy were included in this analysis. Patients with small cell carcinomas were excluded. Recurrence was confirmed by clinical examination including histological analysis or radiologic investigation. For all patients, clinical data on the following characteristics were collected: initial stage, cell type, primary treatment, site of recurrent disease, disease free interval (DFI), chemotherapy regimen, response, and PFS. DFI was defined as the time from the completion of the successful initial treatment to the detection of recurrence. PFS was measured from the start of chemotherapy to the progression of disease. Since most of the patients treated with TC are still alive at the time of this study, we did not include overall survival (OS) as an endpoint in the current study.

Table 2
Non-taxane containing platinum-based chemotherapy (NTP)

Chemotherapy	Reference	Dose of chemotherapy	Number of patients
Single-agent cisplatin	[17]	Cisplatin 50 mg/m^2, iv	2
Single-agent nedaplatin	[18]	Nedaplatin 70 mg/m^2, iv	11
Cisplatin-based doublet	[19]	Cisplatin 50 mg/m^2 on day 1, iv 5-fluorouracil 300 mg/m^2 on day 1–5, iv	1
Nedaplatin-based doublet	[20]	Nedaplatin 70 mg/m^2 on day 1, iv 5-fluorouracil 300 mg/m^2 on day 1–5, iv	10
Cisplatin-based triplet	[21]	Cisplatin 50 mg/m^2 on day 1, iv Ifosphamide 1.5 g/m^2 plus mesna 1 g/m2 on day 1–5, iv Peplomycin 5 mg/patient on day 1–6, im	4
Nedaplatin-based triplet	[22]	Nedaplatin 70 mg/m^2 on day 1, iv Ifosphamide 1.5 g/m^2 plus mesna 1 g/m2 on day 1–5, iv Peplomycin 5 mg/patient on day 1–6, im	3

iv; intravenously.
im; intramuscularly.

Control patients

A nonrandomized control group of patients with recurrent cervical cancer after definitive radiotherapy who had been treated with non-taxane containing platinum-based chemotherapy (NTP) from 1998 to 2005 were also identified through the chart review and served as a historical comparison.

The patients in the historical control had been treated with various chemotherapy regimens. As shown in Table 2, before 2005, in our institution, patients with recurrent cervical cancer were treated with platinum-based non-taxane containing regimens, based on previous reports, which showed significant activities in patients with recurrent cervical cancer [17–22]. Each of the chemotherapy cycles was repeated every 3–4 weeks and continued until either disease progression or complete response for a maximum of 9 courses.

Response and toxicity evaluations

Patients were considered evaluable for response if they had received at least two cycles of chemotherapy or had demonstrated the appearance of a new lesion or significant clinical deterioration that could not be attributed to treatment or other medical conditions after one course of the treatment. The response to treatment was assessed according to the Response Evaluation Criteria in Solid Tumors (RECIST) after every three cycles of each regimen. A complete response (CR) was defined as the disappearance of all target and non-target lesions and no new lesions being documented after two assessments that were at least 4 weeks apart. A partial response (PR) was defined as at least a 30% decrease in the sum of the longest dimension of the target lesions, which was also documented in two assessments that were at

Table 1
Summary of articles on the activity of paclitaxel–carboplatin in cervical cancer

Article		Target disease	Dose of chemotherapy	Cycle	Number of patients	Response			Patients with prior radiotherapy
Author	Year					Number of CR	Number of PR	Response rate (%)	
Piver MS [14]	1999	R or A	Paclitaxel; 135 m^2 carboplatin; 300 mg/m^2	Every 4 weeks	3	1		33.3	2 (66.7%)
Sit AS [12]	2004	R	Paclitaxel; 135–175 m^2 carboplatin; AUC 5	Every 3 weeks	15	4	5	60	14 (93.3%)
Tinker AV [16]	2005	R or A	Paclitaxel; 175 m^2 carboplatin; AUC 5–6	Every 4 weeks	25	5	5	40	23 (92%)
Secord AA [15]	2007	R or A	Paclitaxel; 80 m^2 carboplatin; AUC 2	Day 1, 8, 15 of each 28-day cycle	15		3	20	13 (86.7%)
Moore KN [13]	2007	R	NA	NA	48	12	12	50	43 (89.6%)
Current study		R	Paclitaxel; 175 m^2 carboplatin; AUC 5 or paclitaxel; 80 m^2 carboplatin; AUC 2	Every 4 weeks or Day 1, 8, 15 of each 28-day cycle	28	5	14	67.9	28 (100%)
Total					134	27	39	49	

R; Recurrent cervical cancer, A; Advanced cervical cancer, NA; Not available.

least 4 weeks apart. Progressive disease (PD) was defined as a 20% increase in the longest dimension of the sum of the target lesions or the development of new lesions. Stable disease (SD) implies that none of the above applies. Toxicity related to treatment was graded according to the NCI Common Terminology Criteria for Adverse Events, Version 3.0. For patients who had been treated before the introduction of RECIST or NCI Common Terminology Criteria for Adverse Events, Version 3.0., information related to disease status and toxicity were collected, and response rate and toxicity were retrospectively reevaluated according to these criteria.

Statistical analysis

The differences between the groups with respect to stage, histology, site of recurrence, and prior treatment were assessed using the Fisher's exact Test. The Wilcoxon rank-sum test was used to analyze age and DFI. Response rate and toxicities were also compared using Fisher's exact Test. PFS was calculated using the Kaplan–Meier method and compared by the log-rank test. Multivariate analysis of prognostic variables including the type of chemotherapy (TC or NTP), clinical stage, histology, DFS, site of recurrence, prior chemoradiotherapy, and prior chemotherapy for response was performed using the Cox proportional hazards regression analysis. P values of <0.05 were considered statistically significant.

Results

Patients

Fifty-nine consecutive women with recurrence that were treated either with TC ($n=28$) or NTP ($n=31$) were identified. All patients had previously been treated with primary radiotherapy with curative intent or adjuvant radiotherapy after radical hysterectomy. The clinico-pathologic characteristics of these patients are shown in Table 3. Among the patients treated with TC, the median age at the time of treatment for recurrence was 58. Three patients had stage I disease, 8 had stage II, 8 had stage III, and 9 had stage IV. Twenty-three women (82%) had squamous cell carcinoma, 5 (18%) had adenocarcinoma. Seventeen patients (61%) received concurrent radio-sensitizing cisplatin. The mean and median DFI were 6 and 17 months, respectively. Seven patients (25%) had recurrence within the irradiated field. One patient had prior non-taxane containing platinum-based chemotherapy for recurrent disease. As shown in Table 3, there were no significant differences in patient characteristics. There was also no significant difference with respect to performance status (PS), which is known to be an independent prognostic factor in cervical cancer (data not shown).

Table 3
Patients characteristics

		TC-group ($n=28$)	NTP-group ($n=31$)	P value
		n (%)	n (%)	
Age	Median (Range)	54 (33–75)	53 (33–76)	0.284
Stage	Ib	3 (10.7)	5 (16.1)	0.075
	IIa–b	8 (28.6)	14 (45.2)	
	IIIa–b	8 (28.6)	7 (22.6)	
	IVa	1 (3.5)	2 (6.4)	
	IVb	8 (28.6)	3 (9.7)	
Histology	SCC	23 (82.1)	27 (87.1)	0.723
	Adenocarcinoma	5 (17.9)	4 (12.9)	
DFS (months)	Median	6	6.5	0.609
	Mean	17	23.8	
Site of recurrence	Inside irradiated field	7 (25)	11 (35.5)	0.606
	Outside irradiated field	13 (46.4)	11 (35.5)	
	Both	8 (28.6)	9 (29)	
Prior chemoradiotherapy	Yes	11 (39.3)	5 (16.1)	0.077
	No	17 (60.7)	26 (83.9)	
Prior chemotherapy	Yes	1 (3.6)	2 (6.5)	0.162
	No	27 (96.4)	29 (93.5)	

TC; Paclitaxel-carboplatin, NTP; Non-taxane containing platinum-based chemotherapy.

Table 4
Objective response and toxicities

		TC-group ($n=28$)	NTP-group ($n=31$)	P value
		n (%)	n (%)	
Response	CR+PR	19 (67.9)	7 (22.6)	0.001
	SD	2 (7.1)	5 (16.1)	
	PD	7 (25)	19 (61.3)	
PFS	Median (range)	7 (0–44)	0 (0–14)	0.0001
	Mean	9.25	2	
Toxicity	Patients with Grade 3 toxicity	16 (57.1)	10 (32.2)	1.000
	Patients with Grade 4 toxicity	5 (17.9)	8 (25.8)	

Response rate and progression-free survival

Among the patients that were treated with TC, carboplatin–paclitaxel was administered on a monthly basis (monthly TC) in 26 patients: carboplatin at an AUC of 5–6 and paclitaxel at 175 mg/m^2 given as a 3-h intravenous infusion every 28 days. Two patients were treated on a weekly basis (weekly TC): paclitaxel 80 mg/m^2 and carboplatin at an AUC of 2 on days 1, 8, and 15 of each 28-day cycle. The median course of TC administered was 5 (range: 2–9). As shown in Table 4, the overall response rate was 67.9% (19/28). Five patients showed a CR, 14 showed PR, and 2 patients demonstrated SD. The median PFS was 7 months in the entire group and 10 months in the responders (PR+CR). At the time of this study, 20 out of 28 patients (71.4%) are still alive, and 9 patients (32.1%) have not suffered disease progression after a median follow up period of 14 months.

A subgroup analysis revealed that there were no differences in response rate between the patients previously treated with concurrent cisplatin and the patients previously treated with radiotherapy alone (81% vs. 59%, $p=0.2495$). There were 7 patients who suffered from recurrence inside the irradiated-field, and 13 patients who had recurrence outside. A statistically lower objective response occurred in the patients who had recurrences inside the irradiated-field than in the patients who had recurrences outside the irradiated field (57% vs. 100%, $p=0.0307$). The activity of TC was not significantly affected by histology or clinical stage. Treatment with TC showed a

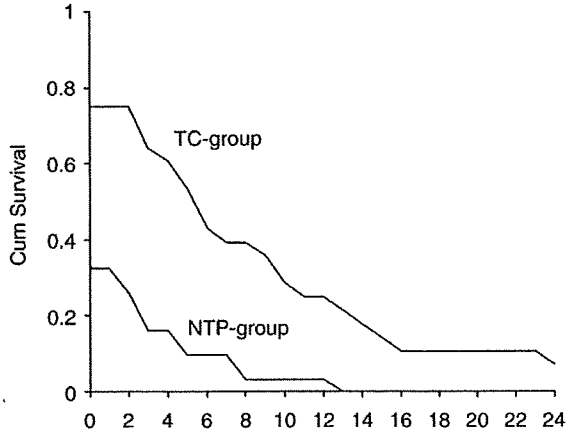

Fig. 1. Progression-free survival among patients in TC-group and control-group.

Table 5
Response by histology, site of recurrence and prior chemoradiotherapy

	TC-group		NTP-group		*P* value
	Number of patients	Patients with response (%)	Number of patients	Patients with response (%)	
Patients with adenocarcinoma	5	4 (80)	4	0 (0)	0.0476
Recurrence inside irradiated-field	7	4 (57.1)	11	2 (18.2)	0.1414
Patients previously treated with chemoradiotherapy	11	9 (81.8)	5	2 (40)	0.2455

TC; Paclitaxel–carboplatin, NTP; Non-taxane containing platinum-based chemotherapy.

response rate of 65% in the patients with SCC and 80% in the patients with adenocarcinoma ($p = 1.00$). Treatment with TC showed a response rate of 63.6% in the patients with stage I–II disease at initial diagnosis, which was almost equal to the 70.6% observed in the patients with stage III–IV disease ($p = 1.00$).

In the NTP-group, as shown in Table 2, various non-taxane containing platinum-based chemotherapy regimens were used. As shown in Table 4 and Fig. 1, the overall response rate was 22.6% with a median PFS of 0 months in the entire group and 4 months in the responders (PR + CR), which was similar to previous reports, which showed a response rate of 20–40% [3,17,18].

When the TC-group was compared with the NTP-group in the univariate analysis, TC was significantly superior in terms of response rate (67.9% vs. 22.6%, $p = 0.001$) and PFS (log-rank; $p < 0.0001$). In a subgroup analysis (Table 5), TC showed a significantly higher response rate than NTP in the patients with adenocarcinoma (80% vs. 0%, $p = 0.0476$). TC also showed a higher response rate for recurrences inside the irradiated-field than NTP; however, this difference did not reach statistical significance (57% vs. 18.2%, $p = 0.1414$). Multivariate analysis demonstrated the site of recurrence ($p = 0.0098$) and chemotherapy regimen ($p = 0.0214$) to be independent prognostic factors for predicting the response to chemotherapy.

Toxicity

Generally, carboplatin–paclitaxel was well tolerated. The most frequently observed toxicity was hematologic toxicity. As shown in Table 4, grade 3 or 4 toxicity was observed in 21 patients (77.8%). All grade 3–4 toxicities observed were neutropenia. Of these, two patients (8%) developed febrile neutropenia. Although grade 1–2 non-hematologic toxicities were commonly observed, there were no grade 3–4 non-hematologic toxicities including gastrointestinal and neurologic toxicities.

In the NTP-group, Grade 3 or 4 toxicities were observed in 18 patients (58%). Hematologic toxicity was common, with 10 patients experiencing grade 3–4 neutropenia and 4 patients experiencing grade 3–4 thrombocytopenia. There were 4 patients with grade 3–4 non-hematologic toxicities, including 3 patients with grade 3 nausea and vomiting and a patient with grade 3 gastrointestinal toxicity.

When compared overall, the incidence of grade 3–4 toxicity did not differ significantly between the two groups (Table 4). Although grade 3 non-hematologic toxicities were observed in 3 patients (9.6%) that had been treated with NTP, there were no grade 3–4 non-hematologic toxicities in the patients treated with TC.

Discussion

Radiotherapy has been a major treatment modality for invasive cervical cancer and has achieved significant treatment outcomes; however, substantial treatment failure still occurs especially in advanced-stage patients [1]. The treatment of recurrent cervical cancer is challenging, and patients with recurrent disease have a dismal prognosis with a 1-year survival rate of between 15% and 20% [5]. Most patients who have recurrences inside the irradiated field are not candidates for further radiotherapy; therefore, systemic chemotherapy is required for these patients. Unfortunately, it has been previously reported that patients with recurrence inside the irradiated field are likely to have a lower response rate than those with recurrence outside of the irradiated-field [23,24], presumably because of the compromised blood supply to the tumor tissue within previously irradiated fields. Survival signals such as AKT [25], HIF-1α [26], and Survivin [27], which are reported to be overexpressed in radioresistant cervical cancer cells, may inversely affect the sensitivity to salvage chemotherapy. Moreover, patients with recurrence inside the irradiated-pelvis, especially recurrence in pelvic side wall, may also have impaired renal function due to ureter obstruction, limiting the use of certain chemotherapeutic agents such as cisplatin.

Based on recent phase III clinical trials, cisplatin-containing combination chemotherapy has become the standard treatment for recurrent cervical cancer [3,6,21,28]. The addition of either paclitaxel [6] or ifosphamide [21] to single-agent cisplatin has improved outcomes in terms of response rate and progression-free survival in patients with advanced or recurrent cervical cancer. The subsequent Gynecologic Oncology Group (GOG) study (protocol GOG 179) is the only trial to date that has demonstrated an improvement in overall survival [28]. Although a combination of cisplatin–topotecan showed a 2.9 month improvement in survival over single-agent cisplatin, further exploration for a more effective combination chemotherapy is necessary.

In our institution, various platinum-based regimens had been tried for patients with recurrent cervical cancer before 2005. Nedaplatin (cis-diammine-glycoplatinum), a derivative of cisplatin developed in Japan, has been reported to have an anti-tumor activity similar to that of cisplatin but a lower renal and gastrointestinal toxicity [29–31]. Although there have been no controlled clinical studies demonstrating the equivalency of these agents, since nedaplatin does not require hydration and therefore can be used in patients with marginal renal function [29], it has been used clinically in Japan as an alternative to cisplatin for patients with recurrent cervical cancer [18]. In this study, 24 out of 31 patients in the historical control were treated with nedaplatin-containing chemotherapies.

In the current study, we have demonstrated that TC is active in patients with recurrent cervical carcinoma after definitive radiotherapy. The response rate was 67.9% with a median progression-free survival of 9.25 months, which are similar to the results of previous reports [12–16]. The overall response rate of NTP was 22.6%. The response rates of nedaplatin- and cisplatin-based chemotherapy were 25% and 14%, respectively (data not shown), which are consistent with previous reports [3,29–31]. Although six different NTP regimens were used, there was no significant difference in response rate between the regimens (data not shown). When compared with the historical control, TC was significantly superior in terms of response rate and PFS. Moreover, TC showed significantly higher activity in patients with adenocarcinoma histology.

As predicted, carboplatin–paclitaxel was well tolerated. The most common toxicity in TC was myelosuppression. Although grade 3–4 hematologic toxicities were observed in 77.8% of patients, the incidence of grade 4 toxicity was low (17.9%), and there were no grade 3–4 non-hematologic toxicities.

In addition to using a less toxic regimen, it is also important to maintain a patient's quality of life. Using agents that can be administered on an outpatient basis is one way physicians can achieve this. As described previously, when combined with cisplatin, paclitaxel is given as a 24-hour infusion in order to reduce its neurologic toxicity [6]. However, when combined with carboplatin, paclitaxel can be administered as a 3-hour infusion [10]. Given the advantages of its convenience and tolerability as well as its significant activity, we believe that paclitaxel–carboplatin is a reasonable treatment option for this patient population.

In conclusion, our data demonstrates that the combination of carboplatin–paclitaxel is active and well tolerated in patients with recurrent cervical cancer after definitive radiotherapy. This study should be interpreted cautiously for several reasons, such as its retrospective design, the relatively small cohort of patients, the heterogeneity of the patient population, and the considerable selection bias exercised by the physicians at our institution in determining which patients with recurrence would be considered for salvage chemotherapy. Moreover, there have been several changes in the pattern of care during the time period covered by this study, including the introduction of chemoradiotherapy as an initial treatment and the improvement of palliative and terminal care. However, we believe that our encouraging results are enough to warrant further investigation of carboplatin–paclitaxel in a future randomized controlled trial as a treatment for recurrent cervical cancer.

Conflict of interest statement
The authors declare that they have no conflicts of interest.

Acknowledgments

We thank Remina Emoto for her secretarial assistance.

References

[1] Cannistra SA, Niloff JM. Cancer of the uterine cervix. N Engl J Med 1996;334:1030–8.
[2] Benedet JL, Odicino F, Maisonneuve P, Beller U, Creasman WT, Heintz AP, Ngan HY, Pecorelli S. Carcinoma of the cervix uteri. Int J Gynaecol Obstet 2003;83 (Suppl 1):41–78.
[3] Long III HJ. Management of metastatic cervical cancer: review of the literature. J Clin Oncol 2007;25:2966–74.
[4] Potter ME, Hatch KD, Potter MY, Shingleton HM, Baker VV. Factors affecting the response of recurrent squamous cell carcinoma of the cervix to cisplatin. Cancer 1989;63:1283–6.
[5] Bonomi P, Blessing JA, Stehman FB, DiSaia PJ, Walton L, Major FJ. Randomized trial of three cisplatin dose schedules in squamous-cell carcinoma of the cervix: a Gynecologic Oncology Group study. J Clin Oncol 1985;3:1079–85.
[6] Moore DH, Blessing JA, McQuellon RP, Thaler HT, Cella D, Benda J, Miller DS, Olt G, King S, Boggess JF, Rocereto TF. Phase III study of cisplatin with or without paclitaxel in stage IVB, recurrent, or persistent squamous cell carcinoma of the cervix: a gynecologic oncology group study. J Clin Oncol 2004;22:3113–9.
[7] Arseneau J, Blessing JA, Stehman FB, McGehee R. A phase II study of carboplatin in advanced squamous cell carcinoma of the cervix (a Gynecologic Oncology Group Study). Invest New Drugs 1986;4:187–91.
[8] McGuire III WP, Arseneau J, Blessing JA, DiSaia PJ, Hatch KD, Given Jr FT, Teng NN, Creasman WT. A randomized comparative trial of carboplatin and iproplatin in advanced squamous carcinoma of the uterine cervix: a Gynecologic Oncology Group study. J Clin Oncol 1990;8:755–6.
[9] Kudelka AP, Siddik ZM, Balat O, Kavanagh JJ. Carboplatin dosimetry in renal failure. J Clin Oncol 1989;7:1748–56.
[10] Ozols RF, Bundy BN, Greer BE, Fowler JM, Clarke-Pearson D, Burger RA, Mannel RS, DeGeest K, Hartenbach EM, Baergen R, Gynecologic Oncology Group. Phase III trial of carboplatin and paclitaxel compared with cisplatin and paclitaxel in patients with optimally resected stage III ovarian cancer: a Gynecologic Oncology Group study. J Clin Oncol 2003;21:3183–5.
[11] Termrungruanglert W, Kudelka AP, Piamsomboon S, Edwards CL, Verschraegen CF, Loyer E, Kavanagh JJ. Remission of recurrent cervical cancer with paclitaxel and carboplatin: a case report and review of literature. Eur J Gynaecol Oncol 1996;17:493–6.
[12] Sit AS, Kelley JL, Gallion HH, Kunschner AJ, Edwards RP. Paclitaxel and carboplatin for recurrent or persistent cancer of the cervix. Cancer Invest 2004;22(3):477–8.
[13] Moore KN, Herzog TJ, Lewin S, Giuntoli RL, Armstrong DK, Rocconi RP, Spannuth WA, Gold MA. A comparison of cisplatin/paclitaxel and carboplatin/paclitaxel in stage IVB, recurrent or persistent cervical cancer. Gynecol Oncol 2007;105:299–303.
[14] Piver MS, Ghamande SA, Eltabbakh GH, O'Neill-Coppola C. First-line chemotherapy with paclitaxel and platinum for advanced and recurrent cancer of the cervix—a phase II study. Gynecol Oncol 1999;75:334–7.
[15] Secord AA, Havrilesky LJ, Carney ME, Soper JT, Clarke-Pearson DL, Rodriguez GC, Berchuck A. Weekly low-dose paclitaxel and carboplatin in the treatment of advanced or recurrent cervical and endometrial cancer. Int J Clin Oncol 2007;12:31–6.
[16] Tinker AV, Bhagat K, Swenerton KD, Hoskins PJ. Carboplatin and paclitaxel for advanced and recurrent cervical carcinoma: the British Columbia Cancer Agency experience. Gynecol Oncol 2005;98:54–8.
[17] Thigpen T, Shingleton H, Homesley H, Lagasse L, Blessing J. Cis-platinum in treatment of advanced or recurrent squamous cell carcinoma of the cervix: a phase II study of the Gynecologic Oncology Group. Cancer 1981;48:899–903.
[18] Noda K, Ikeda M, Yakushiji M, Nishimura H, Terashima Y, Sasaki H, Hata T, Kuramoto H, Tanaka K, Takahashi T, et al. A phase II clinical study of cis-diammine glycolato platinum, 254-S, for cervical cancer of the uterus. Gan To Kagaku Ryoho 1992;19:885–92.
[19] Fuwa N, Kodaira T, Kamata M, Matsumoto A, Furutani K, Tachibana H, Ito Y. Phase I study of combination chemotherapy with 5-fluorouracil (5-FU) and nedaplatin (NDP): adverse effects and eecommended dose of NDP administered after 5-FU. Am J Clin Oncol 2002;25:565–9.
[20] Kaern J, Tropé C, Sundfoer K, Kristensen GB. Cisplatin/5-fluorouracil treatment of recurrent cervical carcinoma: a phase II study with long-term follow-up. Gynecol Oncol 1996;60:387–92.
[21] Bloss JD, Blessing JA, Behrens BC, Mannel RS, Rader JS, Sood AK, Markman M, Benda J. Randomized trial of cisplatin and ifosfamide with or without bleomycin in squamous carcinoma of the cervix: a gynecologic oncology group study. J Clin Oncol 2002;20:1832–7.
[22] Hirabayashi K, Okada E. Combination chemotherapy with 254-S, ifosfamide, and peplomycin for advanced or recurrent cervical cancer. Cancer 1993;71:2769–75.
[23] Friedlander M, Grogan M, U.S. Preventative Services Task Force. Guidelines for the treatment of recurrent and metastatic cervical cancer. Oncologist 2002;7:342–7.
[24] Brader KR, Morris M, Levenback C, Levy L, Lucas KR, Gershenson DM. Chemotherapy for cervical carcinoma: factors determining response and implications for clinical trial design. J Clin Oncol 1998;16:1879–84.
[25] Kim TJ, Lee JW, Song SY, Choi JJ, Choi CH, Kim BG, Lee JH, Bae DS. Increased expression of pAKT is associated with radiation resistance in cervical cancer. Br J Cancer 2006;94:1678–82.
[26] Burri P, Djonov V, Aebersold DM, Lindel K, Studer U, Altermatt HJ, Mazzucchelli L, Greiner RH, Gruber G. Significant correlation of hypoxia-inducible factor-1alpha with treatment outcome in cervical cancer treated with radical radiotherapy. Int J Radiat Oncol Biol Phys 2003;56:494–501.
[27] Bache M, Holzapfel D, Kappler M, Holzhausen HJ, Taubert H, Dunst J, Hänsgen G. Survivin protein expression and hypoxia in advanced cervical carcinoma of patients treated by radiotherapy. Gynecol Oncol 2007;104:139–44.
[28] Long III HJ, Bundy BN, Grendys Jr EC, Benda JA, McMeekin DS, Sorosky J, Miller DS, Eaton LA, Fiorica JV, Gynecologic Oncology Group Study. Randomized phase III trial of cisplatin with or without topotecan in carcinoma of the uterine cervix: a Gynecologic Oncology Group study. J Clin Oncol 2005;23:4626–33.
[29] Kameyama Y, Okazaki N, Nakagawa M, Koshida H, Nakamura M, Gemba M. Nephrotoxicity of a new platinum compound, 254-S, evaluated with rat kidney cortical slices. Toxicol Lett 1990;52:15–24.
[30] Uchida N, Takeda Y, Hojo K, Maekawa R, Sugita K, Yoshioka T. Sequence-dependent antitumour efficacy of combination chemotherapy of nedaplatin, a novel platinum complex, with 5-fluorouracil in an in vivo murine tumour model. Eur J Cancer 1998;34:1796–801.
[31] Sasaki Y, Amano T, Morita M, Shinkai T, Eguchi K, Tamura T, Ohe Y, Kojima A, Saijo N. Phase I study and pharmacological analysis of cis-diammine(glycolato) platinum (254-S; NSC 375101D) administered by 5-day continuous intravenous infusion. Cancer Res 1991;51:1472–7.

Original Research

MR Imaging of Endometrial Carcinoma for Preoperative Staging at 3.0 T: Comparison With Imaging at 1.5 T

Masatoshi Hori, MD, PhD,[1*] Tonsok Kim, MD, PhD,[1] Takamichi Murakami, MD, PhD,[2] Izumi Imaoka, MD, PhD,[2] Hiromitsu Onishi, MD, PhD,[1] Atsushi Nakamoto, MD,[1] Yasuhiro Nakaya, MD, PhD,[1] Kaname Tomoda, MD, PhD,[1] Tateki Tsutsui, MD, PhD,[3] Takayuki Enomoto, MD, PhD,[3] Tadashi Kimura, MD, PhD[3] and Hironobu Nakamura, MD, PhD[1]

Purpose: To prospectively compare magnetic resonance imaging (MRI) at 3.0 T and 1.5 T in the same patients for preoperative evaluation of endometrial carcinoma.

Materials and Methods: Thirty consecutive patients with endometrial carcinoma underwent MRI at both 3.0 T and 1.5 T as well as surgery. Quantitative and qualitative analyses were performed. Two radiologists independently evaluated images. MR findings were compared with surgicopathologic findings.

Results: Image homogeneity of T2-weighted images at 3.0 T was significantly inferior to that at 1.5 T ($P = 0.007$). The scores of image homogeneity and susceptibility artifacts were not significantly different between 3.0 T gadolinium-enhanced imaging and 1.5 T imaging ($P = 0.09$ and 0.36). Kappa statistics showed good interobserver agreement between the two radiologists for local-regional staging on T2-weighted images ($\kappa > 0.6$). The area under the receiver operating characteristic curve (Az) values for T2-weighted imaging in terms of myometrial invasion, cervical invasion, and lymph node metastases were 0.88 (3.0 T) versus 0.91 (1.5 T), 0.84 versus 0.83, and 0.94 versus 0.95 for reader 1, respectively. There were no significant differences between imaging at 3.0 T and at 1.5 T in Az values for either reader ($P > 0.35$).

Conclusion: 3.0 T MRI is an equivalent imaging modality to 1.5 T imaging for presurgical evaluation of endometrial carcinoma, although not significantly superior to 1.5 T imaging.

Key Words: magnetic resonance; high-field strength imaging; 3T; pelvis; uterine neoplasm; diagnostic accuracy
J. Magn. Reson. Imaging 2009;30:621–630.

ENDOMETRIAL CARCINOMA is the most common gynecologic malignancy and the fourth most frequent cancer among females in the United States, with an estimated 40,100 new cases and an estimated 7,470 deaths in 2008 (1). Important prognostic factors are depth of myometrial invasion, histological type, histological grade, vascular space invasion, nodal involvement, and peritoneal cytology (2–4). Preoperative accurate evaluation of the tumor extent could greatly optimize surgical procedure and therapeutic strategy (5–7). The usefulness of magnetic resonance imaging (MRI) in the preoperative assessment of endometrial carcinoma is increasingly being recognized (8–11).

Recently, whole-body 3.0 T MR systems are being increasingly used in clinical settings. Theoretically, 3.0 T imaging offers higher signal-to-noise ratio (SNR) and enhanced spectral separation than does 1.5 T imaging. The gain in SNR can be maintained or traded for either speed or spatial resolution, or both. Compared with 1.5 T, potential outcomes of 3.0 T imaging include changes in tissue T1 and T2 relaxation times, increased magnetic susceptibility effects, increased power deposition, and uncertain efficacy of contrast agents (12). Although 3.0 T imaging has been shown to be more effective than 1.5 T imaging for the brain and musculoskeletal system, its advantages are unclear in the chest, abdomen, and pelvis because of some unique artifacts such as dielectric artifacts (13). These artifacts can deteriorate image quality and potentially lead to inferior diagnostic capability. Thus, 3.0 T imaging may not be adequate for the preoperative assessment of endometrial carcinoma, and this could be a major problem in view of the fact that the number of 3.0 T scanners is increasing worldwide. Although some reports have dealt with the value

[1]Department of Radiology, Osaka University Graduate School of Medicine, Osaka, Japan.
[2]Department of Radiology, Kinki University School of Medicine, Osaka, Japan.
[3]Department of Obstetrics and Gynecology, Osaka University Graduate School of Medicine, Osaka, Japan.
*Address reprint requests to: M.H., Department of Radiology, Osaka University Graduate School of Medicine, D1, 2-2, Yamadaoka, Suita, Osaka 565-0871 Japan. E-mail: mhori@radiol.med.osaka-u.ac.jp
Received March 31, 2009; Accepted June 12, 2009.
DOI 10.1002/jmri.21879
Published online in Wiley InterScience (www.interscience.wiley.com).

of 3.0 T imaging in the female pelvis (14–19), no studies have made a comparative analysis of the efficacy of 3.0 T and 1.5 T imaging in the same patients for evaluating the presurgical stage of endometrial carcinoma.

The purpose of this study was to prospectively compare MRI at 3.0 T and 1.5 T for the same population of patients in terms of their usefulness for the preoperative staging of endometrial carcinoma.

MATERIALS AND METHODS

This study was approved by our Institutional Review Board and written informed consent was obtained from all patients.

Patients

Between October 2006 and December 2007, 53 consecutive women suspected of having endometrial carcinoma were examined with MRI at our hospital. Fifteen patients did not consent to be included in the study, five did not undergo surgery, and three were excluded because the definitive histopathology was not carcinoma (one carcinosarcoma, one ovarian cancer, and one endometrial hyperplasia). The final study population comprised 30 patients (age range, 43–75 years; mean ± standard deviation [SD], 58.7 ± 8.0 years; body weight range, 41.9–69.4 kg; mean ± SD, 53.5 ± 6.7 kg). Six (20%) were premenopausal and 24 (80%) postmenopausal, and all of them underwent hysterectomy 1–57 days (mean, 28.1 ± 13.8 days) after MR examination.

Surgical confirmation of the diagnosis was obtained by means of total abdominal hysterectomy with pelvic lymphadenectomy in 21 patients, total abdominal hysterectomy without pelvic lymphadenectomy in 7, Piver's type II hysterectomy with pelvic lymphadenectomy in 1, Piver's type IV hysterectomy with pelvic lymphadenectomy in 1 (20). Seven patients did not undergo pelvic lymphadenectomy, and it was presumed that the patient had no metastatic lymph nodes based on preoperative computed tomography (CT), MRI, and follow-up CT obtained 6 months after surgery. One of the seven patients underwent chemotherapy after surgery and the other patients did not. Gross evaluation of the degree of myometrial invasion, cervical invasion, and lymph node metastasis and microscopic confirmation were performed by pathologists using the International Federation of Gynecology and Obstetrics criteria. Histologic examination after hysterectomy established that 28 (93.3%) of 30 tumors were endometrioid adenocarcinomas, one (3.3%) was a clear cell adenocarcinoma, and one (3.3%) an adenosquamous cell carcinoma. Grade 1 tumors were diagnosed in 17 (56.7%) patients, grade 2 tumors in seven (23.3%), and grade 3 tumors in six (20.0%).

MR Examination

Imaging was performed using state-of-the-art 3.0 T and 1.5 T MR scanners (Signa Excite HD; GE Healthcare, Milwaukee, WI) operating with software of comparable levels and with 8-channel body array coils. MRI was performed for both 3.0 T and 1.5 T units on the same day within 30-minute intervals. Before the examination all patients received intramuscular administration of 20 mg of butyl-scopolamine to prevent peristalsis artifact except when contraindicated. The order of imaging at either 3.0 T or 1.5 T was randomized. Fifteen patients had their 3.0 T study first (age range, 43–69 years; mean ± SD, 58.5 ± 7.7 years; body weight range, 47.6–69.4 kg; mean ± SD, 55.0 ± 6.6 kg;12 patients had butyl-scopolamine administration), and the remaining 15 patients had their 1.5 T study first (age range, 46–75 years; mean ± SD, 58.9 ± 8.6 years; body weight range, 41.9–62.1 kg; mean ± SD, 52.0 ± 6.7 kg; 14 patients had butyl-scopolamine administration). There were no significant differences in mean age and mean body weight between the two groups (P = 0.88 and 0.23, respectively, unpaired t-test). At 3.0 T, a dielectric pad was placed on the patient's body in order to improve the image homogeneity (21,22). T2-weighted FSE images in oblique sagittal (parasagittal) planes that were parallel to the longitudinal axis of the uterus and in oblique (paraxial or paracoronal) planes that were parallel to the short axis were obtained with a repetition time (TR) of 6000 msec (3.0 T) or 4000 msec (1.5 T), an echo time (TE) of 90 msec, two signals acquired, an echo-train length (ETL) of 18 (3.0 T) or 12 (1.5 T), receiving bandwidth of 62.5 kHz (3.0 T) or 31.2 kHz (1.5 T), and a 512 × 256 matrix. The section thickness was 5 mm with a 1-mm intersection gap and 24-cm field of view. Saturation bands were placed anteriorly, but only for imaging in parasagittal planes, to eliminate the phase-shift artifact caused by subcutaneous fat. Sensitivity encoding techniques were not used. Acquisition time was either 198 seconds (3.0 T) or 184 seconds (1.5 T).

After obtaining T2-weighted images on both 3.0 T and 1.5 T scanners, precontrast T1-weighted and contrast-enhanced dynamic MR images were obtained only on the second scanner in parasagittal planes that were parallel to the longitudinal axis of the uterus. Thus, 15 patients had only 3.0 T dynamic MR images, and the remaining 15 patients had only 1.5 T dynamic MR images. Dynamic images were obtained using T1-weighted 3D gradient echo (LAVA: Liver Acquisition of Volume Acceleration, GE Healthcare) with fat suppression sequences (TR/TE; 4.6/2.3, 12° flip angle, 320 × 192 matrix, field of view 28 cm, receiver bandwidth 62.5 kHz, a parallel imaging reduction factor of 2, one signal acquired, 4-mm section thickness, 4-mm section interval, 36 partitions, 20-sec acquisition time) before and 25, 70, and 120 seconds after intravenous 17 mL gadolinium administration (gadoteridol: ProHance, Eisai, Tokyo, Japan) at a rate of 2 mL/s.

Imaging Analysis

Quantitative Analysis

All images were transferred to a workstation for quantitative analysis. The analysis was performed by one radiologist (M.H.) with 15 years' experience in genitourinary imaging, and was applied to images by using the operator-defined region of interest (ROI) measurements. ROIs were circular and at least 0.15 cm^2 in area. The signal intensities were measured in areas devoid of focal signal-intensity changes and prominent artifacts.

For the T2-weighted imaging, an ROI was drawn to encompass the uterine myometrium (mean area, 0.80 cm^2, range 0.17–1.83 cm^2), junctional zone (mean area, 0.26 cm^2, range 0.15–0.61 cm^2), and tumors (mean area, 2.66 cm^2, range 0.22–11.19 cm^2) whenever possible. We used surgical and pathological records for ROIs placement when needed. The standard deviation of background noise (SD_B) was measured along the phase-encoding direction outside the anterior abdominal wall (mean area, 9.23 cm^2, range 4.40–12.75 cm^2) to calculate the following: myometrium SNR = $SI_{myometrium}/SD_B$, junctional zone SNR = $SI_{junctional\ zone}/SD_B$, tumor SNR = SI_{tumor}/SD_B, tumor-to-junctional zone contrast-to-noise ratio (CNR) = $(SI_{tumor}-SI_{junctional\ zone})/SD_B$, and myometrium-to-junctional zone CNR = $(SI_{myometrium}-SI_{junctional\ zone})/SD_B$, where $SI_{myometrium}$, $SI_{junctional\ zone}$, and SI_{tumor} are the signal intensities of the myometrium, junctional zone, and tumor, respectively.

For the contrast-enhanced dynamic MRI, enhancement rate of the myometrium was calculated with the following equation: Enhancement rate = $(SI_{postcontrast}-SI_{precontrast})/SI_{precontrast}$, where $SI_{precontrast}$ and $SI_{postcontrast}$ are the signal intensities of the myometrium on precontrast images and postcontrast images 70 seconds after gadolinium administration, respectively. SNR and CNR were not assessed for dynamic imaging because the parallel imaging technique was used for the image acquisition and, therefore, SNR or CNR cannot be calculated as a characteristic for the entire image (23).

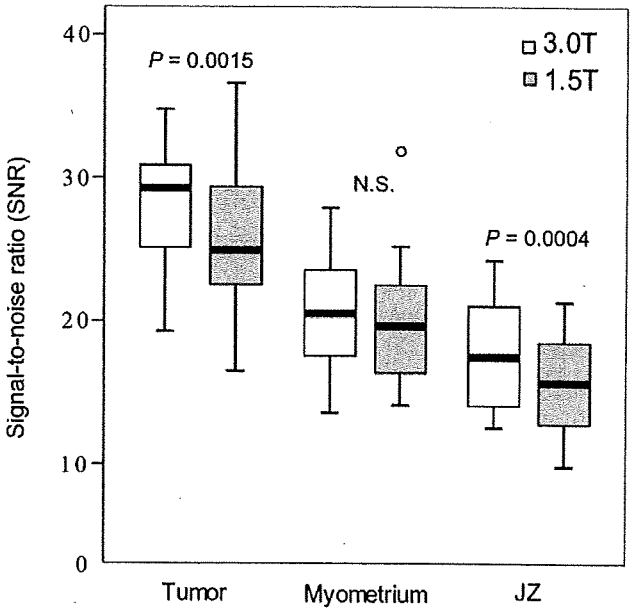

Figure 1. Boxplots show results for SNRs of tumor, myometrium, and junctional zone (JZ) on T2-weighted images. The plots indicate the median (central horizontal line), the 75th quartile (top of box), the 25th quartile (bottom of box), and the smallest and largest nonextreme values (whiskers). Mean values were significantly higher at 3.0 T than at 1.5 T for tumors (P = 0.0015, paired t-test) and junctional zone (P = 0.0004), but not for myometrium (P = 0.23). The mean ratios of the SNR at 3.0 T to those at 1.5 T were 1.12 for tumor, 1.03 for myometrium, and 1.12 for junctional zone. The signal intensity of the myometrium was obtained in all 30 cases. It was also obtained for tumors in 26 cases and for junctional zone in 18 cases. o = outliers.

Qualitative Analysis

Another radiologist (T.Kim) with over 15 years experience in genitourinary imaging reviewed the T2-weighted images obtained with the 3.0 T and 1.5 T units. The review procedure was performed at two separate sessions. The sessions were performed at a 2-week interval. The order of the patients whose images were reviewed was randomized, as was the order in which images obtained with either the 3.0 T or 1.5 T units were reviewed. In other words, images from all 30 patients were reviewed at the first session, but only the images obtained with randomly selected one of the two MR units were reviewed in a given patient at that session. The images obtained with the other MR unit were reviewed at the subsequent session. Image quality was graded in terms of homogeneity and susceptibility artifact using a 4-point scale: 1, unacceptable; 2, poor; 3, fair; and 4, good. Susceptibility artifact was mainly evaluated in terms of gas-related signal loss around the intestine. In the same way, the radiologist evaluated the dynamic MR images of the 30 patients.

Diagnostic Performance Analysis for T2-Weighted Imaging

Two radiologists (T.Kim, I.I.) with over 15 years experience in gynecological MRI independently reviewed the T2-weighted images in both oblique planes obtained with the 3.0 T and 1.5 T units. The review was conducted during two separate sessions at a 2-week interval in the same manner as the image quality analysis. The readers were blinded to the histopathologic findings and which MR unit was used for imaging but knew the age of the patients. The readers were asked to score the images of each patient for the presence of superficial or deep myometrial invasion, cervical invasion, and lymph node metastases. The readers rated the images with one of five confidence levels: 1, definitely absent; 2, probably absent; 3, equivocal; 4, probably present; and 5, definitely present. At the time of scoring the readers were aware that sensitivity or specificity calculations would be performed considering the confidence rating of 4 or 5 as a positive diagnosis. These assessments were made on the basis of established MR criteria. First, myometrial invasion was diagnosed when the junctional zone was disrupted and a mass had invaded the myometrium. When no junctional zone was observed, irregularity of the endometrial–myometrial interface was interpreted as a sign of myometrial invasion. When signal intensity of the tumor extended into the outer half of myometrium, deep myometrial invasion was diagnosed. Second, cervical invasion was diagnosed when an abnormal signal intensity mass within the endocervical canal and/or disruption of the normal low-signal-intensity cervical stroma was observed on T2-weighted images. And third, lymph node metastasis was made when enlarged regional lymph nodes more than 1 cm in minimal diameter were identified.

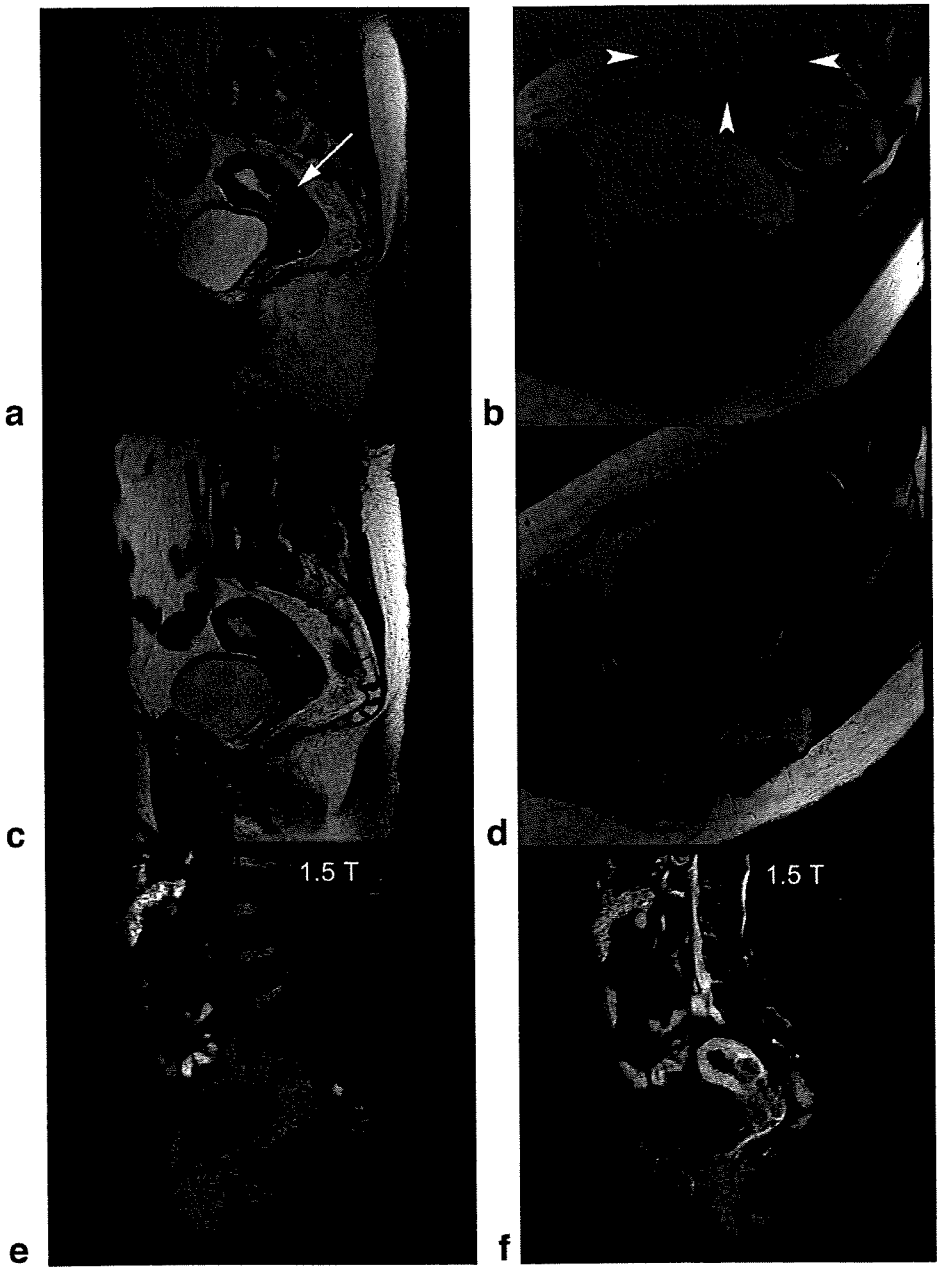

Figure 2. MR images of a 69-year-old woman with endometrial carcinoma (endometrioid adenocarcinoma, grade 1). **a,b:** T2-weighted fast spin-echo images in (a) the parasagittal plane of the uterus and (b) paraxial plane obtained at 3.0 T (6000/90, 18-echo train length) clearly show the tumor with deep myometrial invasion (arrow), which was confirmed by surgicopathologic findings. **c,d:** T2-weighted fast spin-echo images in (c) the parasagittal plane of the uterus and (d) paraxial plane obtained at 1.5 T (4000/90, 12-echo train length) show the same findings. Signal intensity of the tumor at 3.0 T is higher than that at 1.5 T, while image homogeneity is slightly better with 1.5 T imaging than 3.0 T imaging. Signal loss artifact due to dielectric effects is seen on the image at 3.0 T (arrowheads). **e,f:** T1-weighted 3D gradient echo images (4.6/2.3, 12°) at 1.5 T in the parasagittal plane obtained (e) before and (f) 70 seconds after contrast injection show slightly better image homogeneity compared to those at 3.0 T (see Fig. 5).

Statistical Analysis

A paired *t*-test was used for statistical comparison of SNRs and CNRs on 3.0 T and 1.5 T T2-weighted images. An unpaired *t*-test was used for comparison of enhancement rate on 3.0 T and 1.5 T dynamic MR images. The Wilcoxon signed-rank test was used for statistical comparison of 4-point scale scores for image quality of T2-weighted imaging. The Mann–Whitney test was used for statistical comparison of 4-point scale scores for image quality of dynamic MRI.

T2-weighted MRI findings were compared with surgicopathologic findings. Sensitivity, specificity, positive predictive value (PPV), negative predictive value (NPV), and diagnostic accuracy of both 3.0 T and 1.5 T imaging were calculated for diagnosis of myometrial invasion, cervical invasion, and lymph node metastases. For the analyses, only two classifications were used for depth of myometrial invasion: absent or less than 50% and 50% or more, because patients with 50% or greater myometrial invasion are at much greater risk for pelvic and lumboaortic lymph node metastases (3). These values were determined by using confidence scores of 4 or 5 indicating a positive diagnosis. These diagnostic parameters were expressed with a 95% confidence interval (CI). McNemar's test was used for statistical comparison of sensitivity and specificity. Regarding the 5-point scale for image interpretation evaluation, interobserver agreement between the two readers and intermodality agreement between 3.0 T imaging and 1.5 T imaging were determined by calculating the weighted κ

values (quadratic weighting), with κ = 0 indicating poor, κ = 0.01–0.20 slight, κ = 0.21–0.40 fair, κ = 0.41–0.60 moderate, κ = 0.61–0.80 good, and κ = 0.81–1.00 excellent agreement (24).

Furthermore, receiver operating characteristic (ROC) analysis was performed to evaluate diagnostic performance of T2-weighted imaging in relation to the presence of deep myometrial invasion, cervical invasion, and lymph node metastases. An ROC curve was fitted to each reader's confidence rating by using a maximum-likelihood estimation program (ROCKIT 0.9B; C.E. Metz, University of Chicago, Chicago, IL, 1998). The diagnostic performance was then estimated by calculating the area under the ROC curve (Az). The univariate Z-score test was performed to evaluate the significance of the difference between the Az values.

For all statistical analyses other than ROC analysis, a software package (SPSS 11.0 for Windows; Chicago, IL) was used. A *P*-value less than 0.05 was considered to indicate a statistically significant difference.

RESULTS

Quantitative Analysis

In the evaluation of T2-weighted imaging the signal intensity of the myometrium was obtained in all 30 cases. It was also obtained for tumors in 26 cases and for junctional zone in 18 cases. Tumors could barely be identified in four, and junctional zone could not be clearly observed in 12 cases. There were no cases in which visualization of junctional zone or tumor was discordant between 3.0 T and 1.5 T. The mean SNRs of tumors ($P = 0.0015$) and junctional zones ($P = 0.0004$) at 3.0 T were significantly higher than those at 1.5 T (Figs. 1, 2). There were no significant differences in myometrium SNR ($P = 0.23$), tumor-to-junctional zone CNR ($P = 0.15$), and myometrium-to-junctional zone CNR ($P = 0.32$) (Fig. 3). The mean ratios of the SNR at 3.0 T to those at 1.5 T were 1.12 (95% CI, 1.06–1.18) for tumors, 1.03 (0.98–1.08) for myometrium, and 1.12 (1.07–1.18) for junctional zones.

In the evaluation of dynamic MRI, there was no significant difference in enhancement rate of the myometrium between imaging at 3.0 T and 1.5 T ($P = 0.45$) (Figs. 2, 4, 5).

Qualitative Analysis

The results of the qualitative analysis in terms of image homogeneity and susceptibility artifacts are given in Tables 1 and 2. The score for image homogeneity on T2-weighted images at 3.0 T was inferior to that at 1.5 T, with a statistically significant difference ($P = 0.007$) (Figs. 2, 6). The score for susceptibility artifacts on T2-weighted images at 3.0 T was also slightly inferior to that at 1.5 T, but without statistical significance ($P = 0.29$). The score for image homogeneity on dynamic MR images at 3.0 T was slightly inferior to that at 1.5 T, but without statistical significance ($P = 0.09$) (Figs. 2, 5). There was no statistically significant difference between the score for susceptibility artifacts on dynamic MRI between 3.0 T and 1.5 T ($P = 0.36$).

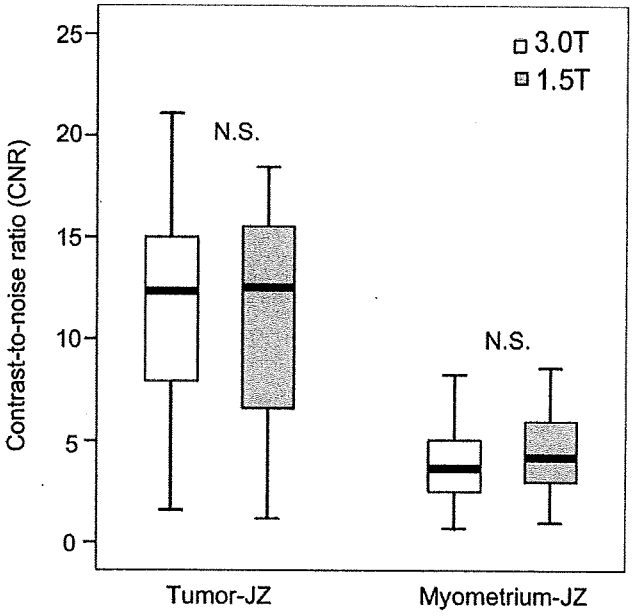

Figure 3. Boxplots show results for tumor-to-junctional zone CNR ($n = 17$) and myometrium-to-junctional zone CNR ($n = 18$) on T2-weighted images. The plots indicate the median (central horizontal line), the 75th quartile (top of box), the 25th quartile (bottom of box), and the smallest and largest nonextreme values (whiskers). There were no significant differences in either values between 3.0 T MRI and 1.5 T MRI ($P = 0.15$ and $P = 0.32$, respectively, paired *t*-test).

Diagnostic Performance Analysis for T2-Weighted Imaging

The results of T2-weighted MRI assessment of the depth of myometrial invasion (absent, 3; <50%, 17; ≥50%, 10) are given in Table 3. According to surgicopathologic data, myometrial invasion was correctly assessed in 15 and 15 (50% and 50%; 3.0 T and 1.5 T, respectively) patients, was underestimated in 12 and 12 (40% and 40%), and overestimated in 3 and 3 (10% and 10%) by reader 1. The corresponding values for reader 2 were 15 and 14 (50% and 47%), 14 and 13 (47% and 43%), and 1 and 3 (3% and 10%).

The Az, sensitivity, specificity, accuracy, PPV, and NPV values assessed by both readers of each of the imagings for the diagnosis of myometrial invasion, cervical invasion (absent, 23; present, 7), and lymph node metastases (absent, 26; present, 4) are given in Table 4. T2-weighted MRI helped make the correct assessment in 85%–95% of patients with myometrial invasion of less than 50% and in 60%–80% of patients with myometrial invasion of 50% or more. There were no significant differences between imaging at 3.0 T and at 1.5 T in Az, sensitivity or specificity values for both readers ($P > .35$, for all comparison pairs).

The κ values for diagnosis of deep myometrial invasion, cervical invasion, and lymph node metastases for the two readers and those values for 3.0 T and 1.5 T T2-weighted imaging are given in Table 5. These values correspond to good to excellent agreement.

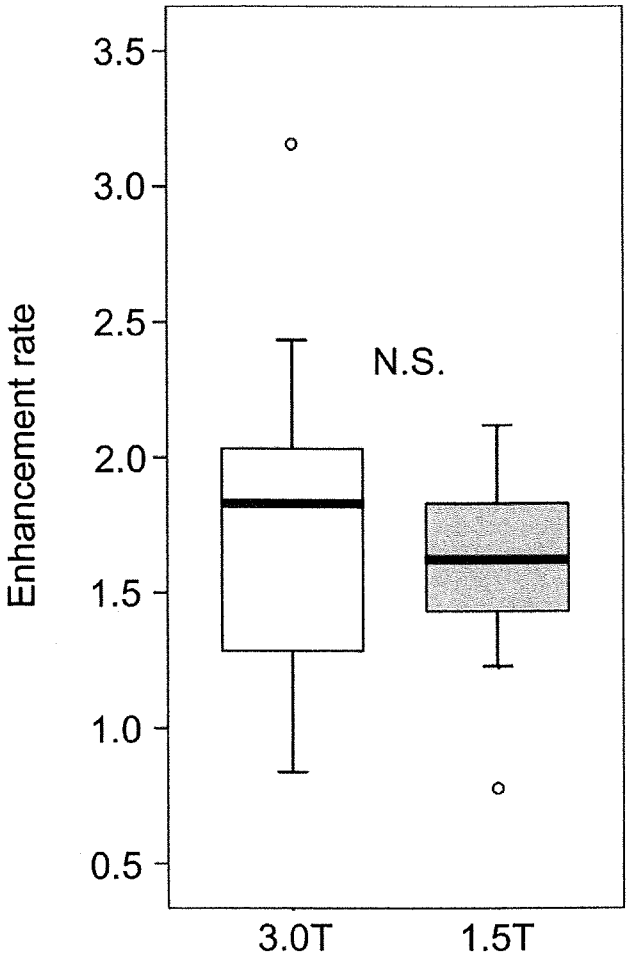

Figure 4. Boxplots show results for enhancement rate of the myometrium on contrast-enhanced T1-weighted images. The plots indicate the median (central horizontal line), the 75th quartile (top of box), the 25th quartile (bottom of box), and the smallest and largest nonextreme values (whiskers). There was no significant difference in mean values between 3.0 T MRI and 1.5 T MRI (P = 0.45, unpaired t-test). o = outliers.

Table 1
Results of Scores for Image Quality With 3.0 T and 1.5 T T2-Weighted MRI in 30 Patients

Score	Image homogeneity [P = 0.007]		Susceptibility artifact [P = 0.29]	
	3.0T	1.5T	3.0T	1.5T
4	8 (26.7)	16 (53.3)	12 (40.0)	16 (53.3)
3	21 (70.0)	14 (46.7)	16 (53.3)	12 (40.0)
2	1 (3.3)	0 (0.0)	2 (6.7)	2 (6.7)
1	0 (0.0)	0 (0.0)	0 (0.0)	0 (0.0)

Data in parentheses are percentages.
Image quality was graded in terms of homogeneity and susceptibility artifact using a 4-point scale: 1, unacceptable; 2, poor; 3, fair; and 4, good.
P-values in square brackets were calculated with the Wilcoxon signed-rank test for statistical comparison of scores between 3.0 T and 1.5 T MRI.

DISCUSSION

3.0 T MRI of the abdomen and pelvis in clinical settings has been introduced recently. The SNR can be expected to be twice as high at 3.0 T as at 1.5 T. This higher SNR could be theoretically used to obtain higher temporal or spatial resolution imaging or a reduction in scan time. For this reason, 3.0 T imaging has established applications in the neuroradiologic field (25,26). However, there are many problems associated with 3.0 T imaging particularly for the abdomen and pelvis (13,27,28). These problems include 1) prolonged T1 relaxation time, although somewhat shortened T2 relaxation time, 2) radiofrequency inhomogeneity, 3) increased specific absorption rate, 4) larger chemical shift, and 5) larger susceptibility effect. As a result, the advantages of a higher magnetic field are not directly applicable to the areas of the abdomen or pelvis. There are a few reports on the role of 3.0 T imaging of the female pelvis (14–19), and only one reported study investigated the capability of 3.0 T imaging for the preoperative evaluation of myometrial invasion in endometrial carcinoma (18). In the latter, the diagnostic accuracy of 3.0 T imaging was found to be equivalent to the highest accuracy values reported in the literature for 1.5 T imaging, although no direct comparison was made for the same population of patients in that study. To the best of our knowledge, our study is the first to directly compare the efficacy of 3.0 T imaging for evaluating the presurgical stage of endometrial carcinoma with that of state-of-the-art 1.5 T imaging. Our results show that, compared with 1.5 T

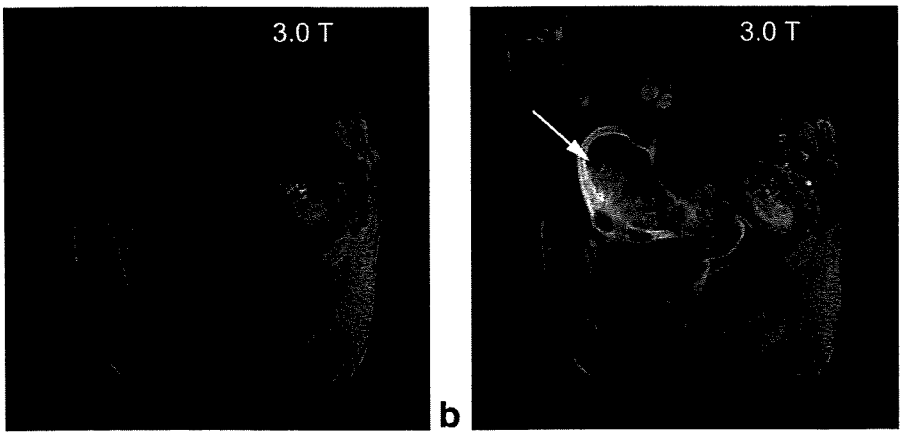

Figure 5. MR images of a 71-year-old woman with endometrial carcinoma (endometrioid adenocarcinoma, grade 3, arrow). T1-weighted 3D gradient echo images (4.6/2.3, 12°) at 3.0 T in the parasagittal plane obtained **(a)** before and **(b)** 70 seconds after contrast injection show excellent contrast enhancement but slightly inferior image homogeneity compared to those at 1.5 T (see Fig. 2).

Table 2
Results of Scores for Image Quality With 3.0 T and 1.5 T Dynamic MRI in 30 Patients

Score	Image homogeneity [P = 0.09]		Susceptibility artifact [P = 0.36]	
	3.0T	1.5T	3.0T	1.5T
4	1 (6.7)	2 (13.3)	1 (6.7)	0 (0.0)
3	9 (60.0)	12 (80.0)	10 (53.3)	14 (93.3)
2	5 (33.3)	1 (6.7)	4 (6.7)	1 (6.7)
1	0 (0.0)	0 (0.0)	0 (0.0)	0 (0.0)

Data in parentheses are percentages.
Image quality was graded in terms of homogeneity and susceptibility artifact using a 4-point scale: 1, unacceptable; 2, poor; 3 fair; and 4, good.
P-values in square brackets were calculated with the Mann-Whitney test for statistical comparison of scores between 3.0 T and 1.5 T MRI.

imaging, 3.0 T imaging improved tumor SNR by around 12%, yielded slightly inferior image homogeneity, and showed equivalent diagnostic capability for the presurgical evaluation of endometrial carcinoma on T2-weighted images. It was also showed that 3.0 T imaging has equivalent enhancement rate and similar image quality in terms of image homogeneity and susceptibility artifacts on dynamic MRI compared with 1.5 T imaging.

It is important to determine the depth of myometrial invasion preoperatively because it is directly related to the prognosis (5). Accurate evaluation could also help in planning the extent of lymphadenectomy, because patients with 50% or greater myometrial invasion are at much greater risk for pelvic and lumboaortic lymph node metastases compared with patients with myometrial invasion that is absent or less than 50% (3). The assessment of cervical invasion is also of clinical importance, because a tumor has a tendency to invade and metastasize to the parametrium if the tumor invades the uterine cervix. A tumor confined within the endometrium may be staged by simple hysterectomy or laparoscopically assisted vaginal hysterectomy (6). In cases with cervical invasion, however, radical surgery, additional radiation therapy, or both are required. In our study we investigated the efficacy of T2-weighted MRI at 3.0 T and 1.5 T in terms of preoperative evaluation of those important factors.

The values we used for some imaging parameters, that is, TR, ETL, and the receiver bandwidth, were different between 3.0 T T2-weighted imaging and 1.5 T imaging. Although optimal parameters for imaging may differ between 3.0 T and 1.5 T, many radiologists use the same parameters for both (14). The MR signal intensity (S) for spin-echo sequence is generally obtained with the following equation:

$$S \propto M\left[1 - \exp\left(\frac{-TR}{T_1}\right)\right]\exp\left(\frac{-TE}{T_2}\right), \quad [1]$$

where T_1 and T_2 are T1 and T2 relaxation times.

T1 relaxation times are longer at 3.0 T than at 1.5 T (29,30); reportedly the T1 relaxation times are 14% longer at 3.0 T than at 1.5 T for endometrium and 42% for the uterine cervix (30). Therefore, we used longer TR by 50% for T2-weighted imaging at 3.0 T compared to that at 1.5 T. We also increased ETL by 50% at 3.0 T to maintain practical imaging times. Moreover, to maintain the equivalent degree of chemical shift misregistration, we doubled the receiver bandwidth at 3.0 T to reduce the degree of misregistration. However, this could lead to an ≈30% reduction in SNR (13). We used the same TEs of 90 msec for 3.0 T and 1.5 T imaging because there is controversy as to whether T2 relaxation times differ between 3.0 T and 1.5 T (13). One study concluded that T2 relaxation time is independent of the main magnetic field strength (29). However, a recent study suggested that T2 relaxation times differ between 3.0 T and 1.5 T (30).

Contrast enhancement effect of gadolinium agents is theoretically higher at 3.0 T than at 1.5 T because longer baseline relaxation times at 3.0 T yield a stronger T1 reduction (31). This has been demonstrated in vivo for imaging brain tumors (32). However, our results showed no significant differences between 3.0 T and 1.5 T in enhancement rate of the myometrium on gadolinium-enhanced T1-weighted images. This is in agreement with reported results on contrast-enhanced breast MRI, in which researchers showed 1.5 T imaging had stronger contrast enhancement for breast tumors

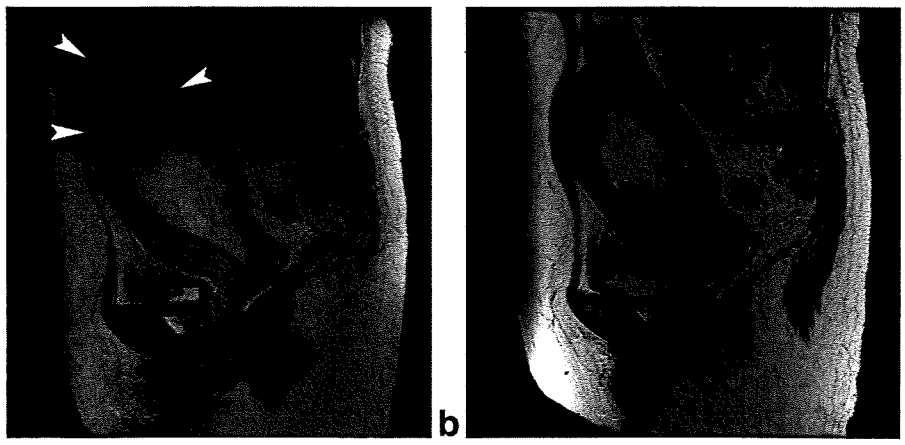

Figure 6. T2-weighted fast spin-echo MR images of a 61-year-old woman with endometrial carcinoma (adenosquamous cell carcinoma, grade 3). a: Parasagittal image at 3.0 T (6000/90, 18-echo train length) shows signal loss artifact around the uterine fundus (arrowheads). b: Parasagittal image at 1.5 T (4000/90, 12-echo train length) does not show the artifact. Image homogeneity is obviously better with 1.5 T than with 3.0 T imaging.

Table 3
Depth of Myometrial Invasion Between T2-Weighted MRI and Surgicopathologic Specimen

T2-weighted MR Findings	Surgicopathologic specimen			
	No myometrial invasion (3.0T/1.5T)	<50% myometrial invasion (3.0T/1.5T)	≥50% myometrial invasion (3.0T/1.5T)	Total (3.0T/1.5T)
Reader 1				
No myometrial invasion	3/3	9/10	1/1	13/14
<50% myometrial invasion	0/0	5/4	2/1	7/5
≥50% myometrial invasion	0/0	3/3	7/8	10/11
Total	3	17	10	30
Reader 2				
No myometrial invasion	3/3	11/9	2/3	16/15
<50% myometrial invasion	0/0	5/5	1/1	6/6
≥50% myometrial invasion	0/0	1/3	7/6	8/9
Total	3	17	10	30

compared to 3.0 T imaging (33). Kuhl et al (31) suggested that better contrast enhancement at 3.0 T might not be the case in body applications, and speculated that the reason would probably be the inhomogeneous radiofrequency penetration in body tissues that might go along with regionally reduced flip angles, which could cause a regionally reduced T1 contrast within an image.

Some limitations need to be taken into consideration. First, one criticism of our study could be related to the fact that we compared only T2-weighted images for the diagnostic performance analysis. Although T2-weighted imaging plays an important role in diagnosing endometrial carcinoma, contrast-enhanced dynamic MRI is also important. It is useful for evaluating myometrial invasion, especially when junctional zone is

Table 4
Statistical Values for Assessment of Myometrial Infiltration, Cervical Invasion, and Lymph Node Metastases With T2-Weighted MRI

		Az	Sensitivity (%)	Specificity (%)
Reader 1				
Myometrial invasion	3.0T	0.88	70 (7/10) [42, 98]	85 (17/20) [69, 100]
	1.5T	0.91	80 (8/10) [55, 100]	85 (17/20) [69, 100]
Cervical invasion	3.0T	0.84	43 (3/7) [6, 80]	100 (23/23) [100, 100]
	1.5T	0.83	43 (3/7) [6, 80]	91 (21/23) [80, 94]
Lymph node metastases	3.0T	0.94	75 (3/4) [33, 100]	92 (24/26) [82, 100]
	1.5T	0.95	75 (3/4) [33, 100]	92 (24/26) [82, 100]
Reader 2				
Myometrial invasion	3.0T	0.90	70 (7/10) [42, 98]	95 (19/20) [85, 100]
	1.5T	0.82	60 (6/10) [30, 90]	85 (17/20) [69, 100]
Cervical invasion	3.0T	0.84	43 (3/7) [6, 80]	91 (21/23) [80, 94]
	1.5T	0.76	43 (3/7) [6, 80]	91 (21/23) [80, 94]
Lymph node metastases	3.0T	0.85	50 (2/4) [1, 99]	88 (23/26) [76, 100]
	1.5T	0.94	75 (3/4) [33, 100]	92 (24/26) [82, 100]

		Accuracy (%)	PPV (%)	NPV (%)
Reader 1				
Myometrial invasion	3.0T	80 (24/30) [66, 94]	70 (7/10) [42, 98]	85 (17/20) [69, 100]
	1.5T	83 (25/30) [70, 97]	73 (8/11) [46, 99]	89 (17/19) [76, 100]
Cervical invasion	3.0T	87 (26/30) [75, 99]	100 (3/3) [100, 100]	85 (23/27) [72, 99]
	1.5T	80 (24/30) [66, 94]	60 (3/5) [17, 100]	84 (21/25) [70, 98]
Lymph node metastases	3.0T	90 (27/30) [79, 100]	60 (3/5) [17, 100]	96 (24/25) [88, 100]
	1.5T	90 (27/30) [79, 100]	60 (3/5) [17, 100]	96 (24/25) [88, 100]
Reader 2				
Myometrial invasion	3.0T	87 (26/30) [75, 99]	88 (7/8) [65, 100]	86 (19/22) [72, 100]
	1.5T	77 (23/30) [62, 92]	67 (6/9) [36, 97]	81 (17/21) [64, 98]
Cervical invasion	3.0T	80 (24/30) [66, 94]	60 (3/5) [17, 100]	84 (21/25) [70, 98]
	1.5T	80 (24/30) [66, 94]	60 (3/5) [17, 100]	84 (21/25) [70, 98]
Lymph node metastases	3.0T	83 (25/30) [70, 97]	40 (2/5) [0, 83]	92 (23/25) [81, 100]
	1.5T	90 (27/30) [79, 100]	60 (3/5) [17, 100]	96 (24/25) [88, 100]

Az, area under the ROC curve; PPV, positive predictive value; NPV, negative predictive value. Numbers in parentheses are used for calculation. Numbers in square brackets are 95% CIs. For the analyses, only two classifications were used for myometrial invasion: absent or less than 50% and 50% or more.
There were no statistically significant differences between imaging at 3.0 T and at 1.5 T in Az, sensitivity, and specificity values for both readers ($P > 0.35$, for all comparison pairs).

Table 5
κ Values for Interobserver and Intermodality Agreement (T2-Weighted Imaging)

κ value	Interobserver		Intermodality	
	3.0T	1.5T	Reader 1	Reader 2
Myometrial invasion	0.66	0.67	0.86	0.78
Cervical invasion	0.77	0.76	0.83	0.72
Lymph node metastases	0.64	0.74	0.83	0.66

Values were calculated from the 5-point scale scores assigned by the two readers for the presence of deep myometrial invasion, cervical invasion, and lymph node metastases using weighted κ statistics (quadratic weighting) to evaluate interobserver agreement between the two readers and intermodality agreement between 3.0 T imaging and 1.5 T T2-weighted imaging.

poorly visible on T2-weighted images (9). Kinkel et al (8) showed that contrast-enhanced MRI had a higher performance compared to nonenhanced MRI in diagnosing endometrial carcinoma in a meta-analysis. However, we thought our patients would be at greater risk if they were injected twice with contrast material to compare the efficacy of dynamic MRI at 3.0 T and 1.5 T. We therefore focused on T2-weighted imaging in our present study. Our study showed that diagnostic performance of T2-weighted images was not significantly different between 3.0 T and 1.5 T imaging, and that there were no significant differences in image quality or the degree of contrast enhancement in gadolinium-enhanced imaging. Therefore, we think that 3.0 T imaging can be regarded as a good diagnostic technique for presurgical evaluation of endometrial carcinoma.

Patients received intramuscular administration of butyl-scopolamine to prevent peristalsis artifact before the examination. This could be another bias for the comparison of the images, because butyl-scopolamine could not be effective up to 30 minutes, which were the intervals between 3.0 T and 1.5 T imaging. However, we tried to minimize this bias by randomizing the order of imaging.

We used a fixed dose of 17 mL of contrast material in this study. This could be another limitation for comparison of the degree of contrast enhancement because the degree of enhancement would also depend on the dose per body weight. However, there were no significant differences in mean body weight between the two groups in our study. Although other factors such as cardiac output and menstrual cycle could affect the degree of contrast enhancement, we could not match those factors between the two groups.

Another criticism of this study could be a lack of accuracy in the comparison of MRI and pathologic findings, especially in terms of lymph node metastases. Seven patients did not undergo pelvic lymphadenectomy. This means that our results for the diagnosis of lymph node metastases may be somewhat inaccurate. However, this is unlikely to be a prominent drawback because the purpose of our study was to compare MRI capability at 3.0 T and 1.5 T. Our study was also limited by a relatively small sample size of 30 patients. We think that larger sample sizes are required to evaluate the diagnostic performance with greater precision.

We did not use special techniques such as higher spatial resolution imaging at 3.0 T. There was a possibility that we could have better image quality and have higher diagnostic performance by using special techniques for 3.0 T imaging. However, we did not take this approach in our study because the gain in SNR was not so prominent for 3.0 T imaging in our preliminary experience. By using recent techniques such as parallel excitation (multitransmitter system) (34) or phased array transmit coils (35), image homogeneity may be improved, and therefore there is a possibility that diagnostic performance of 3.0 T imaging can be much better than that in this study.

In conclusion, 3.0 T MRI is an equivalent imaging modality to 1.5 T imaging for presurgical evaluation of endometrial carcinoma, although not significantly superior to 1.5 T imaging. New imaging techniques which make effective use of the inherently higher SNR at 3.0 T could make 3.0 T imaging more advantageous in the future.

REFERENCES

1. American Cancer Society. Cancer facts and figures 2008. Atlanta: American Cancer Society; 2008:4.
2. Boronow RC, Morrow CP, Creasman WT, et al. Surgical staging in endometrial cancer: clinical-pathologic findings of a prospective study. Obstet Gynecol 1984;63:825–832.
3. Creasman WT, Morrow CP, Bundy BN, Homesley HD, Graham JE, Heller PB. Surgical pathologic spread patterns of endometrial cancer. A Gynecologic Oncology Group study. Cancer 1987;60:2035–2041.
4. Creutzberg CL, van Putten WL, Koper PC, et al. Surgery and postoperative radiotherapy versus surgery alone for patients with stage-1 endometrial carcinoma: multicentre randomised trial. PORTEC Study Group. Post Operative Radiation Therapy in Endometrial Carcinoma. Lancet 2000;355:1404–1411.
5. Grigsby PW, Perez CA, Kuten A, et al. Clinical stage I endometrial cancer: prognostic factors for local control and distant metastasis and implications of the new FIGO surgical staging system. Int J Radiat Oncol Biol Phys 1992;22:905–911.
6. Schlaerth AC, Abu-Rustum NR. Role of minimally invasive surgery in gynecologic cancers. Oncologist 2006;11:895–901.
7. Koyama T, Tamai K, Togashi K. Staging of carcinoma of the uterine cervix and endometrium. Eur Radiol 2007;17:2009–2019.
8. Kinkel K, Kaji Y, Yu KK, et al. Radiologic staging in patients with endometrial cancer: a meta-analysis. Radiology 1999;212:711–718.
9. Manfredi R, Mirk P, Maresca G, et al. Local-regional staging of endometrial carcinoma: role of MR imaging in surgical planning. Radiology 2004;231:372–378.
10. Nakao Y, Yokoyama M, Hara K, et al. MR imaging in endometrial carcinoma as a diagnostic tool for the absence of myometrial invasion. Gynecol Oncol 2006;102:343–347.
11. Chung HH, Kang SB, Cho JY, et al. Accuracy of MR imaging for the prediction of myometrial invasion of endometrial carcinoma. Gynecol Oncol 2007;104:654–659.
12. Edelman RR, Salanitri G, Brand R, et al. Magnetic resonance imaging of the pancreas at 3.0 Tesla: qualitative and quantitative comparison with 1.5 Tesla. Invest Radiol 2006;41:175–180.
13. Merkle EM, Dale BM. Abdominal MRI at 3.0 T: the basics revisited. AJR Am J Roentgenol 2006;186:1524–1532.